Aquaculture 578 (2024) 740109

Contents lists available at ScienceDirect

Aquaculture

journal homepage: www.elsevier.com/locate/aquaculture

Hydrological connectivity controls on the dynamics of particulate organic matter in a semi-enclosed mariculture bay

Aiqin Han [a,*], Jin-Yu Terence Yang [b], Mengli Chen [c], Zhenzhen Zheng [d], Xijie Yin [a], Hui Lin [a,*], Min Nina Xu [d], Shuh-Ji Kao [b,d]

[a] Third Institute of Oceanography, Ministry of Natural Resources, Xiamen, China
[b] State Key Laboratory of Marine Environmental Science, College of Ocean and Earth Sciences, Xiamen University, Xiamen, China
[c] Tropical Marine Science Institute, National University of Singapore, Singapore
[d] State Key Laboratory of Marine Resource Utilization in South China Sea, Hainan University, Haikou, China

ARTICLE INFO

Keywords:
Carbon and nitrogen stable isotopes
Organic matter
Isotopic mixing model
Oxygen consumption and production
Mariculture
Semi-enclosed coastal bay

ABSTRACT

Semi-enclosed bay provides favorable conditions for mariculture, however, mariculture activities can disrupt hydrological connectivity of river-coastal continuum and create a bioreactor for particulate organic matter (POM). The impacts of increasing mariculture activities on POM dynamics, including sources, transportation, and transformation, associated dissolved oxygen and nutrients in semi-enclosed bays remain unclear. This study investigated carbon and nitrogen contents, as well as the stable isotopic compositions of POM ($\delta^{13}C_{POC}$ and $\delta^{15}N_{PN}$) in a semi-enclosed bay, Sansha Bay, which is the largest mariculture bay for large yellow croaker in China and is influenced by riverine input and nearshore coastal waters. Our findings revealed that, spatially, riverine POM dominated along main channel that connects river inlet and bay outlet under the influence of water mixing (C:N ratios ~ 5.7–15.8, $\delta^{13}C_{POC}$ ~ −21‰–24‰, and $\delta^{15}N_{PN}$ ~ 13‰-17‰). On top of water mixing, autochthonous POM dominates in off-main channel (C:N ratio 5–9, $\delta^{13}C_{POC}$ -21‰–17‰, and $\delta^{15}N_{PN}$ 7.0‰-8.5‰). Using a three end-member isotopic mixing model, our data shows that the POM in main channel comprises ~ 90% of riverine POM and ~ 10% of phytoplankton production, while in off-main channel, ~ 59% of POM was contributed by autochthonous phytoplankton production and the rest ~ 41% was sourced from main channel. Furthermore, riverine POM degradation consumes oxygen along main channel, forming consistent with the classic Redfield stoichiometry of aerobic respiration (N:O_2, ~ 0.13 ± 0.02). In contrast, in off-main channel where water exchange is slower, the degradation of fish feed regenerates dissolved inorganic nitrogen, which subsequently stimulates phytoplankton production, leading to oxygen production following the canonical Redfield stoichiometry of phytoplankton photosynthesis (N:O_2, ~ 0.10 ± 0.01). Our results highlight the influence of hydrological connectivity, superimposed by mariculture activity, in shaping POM biogeochemistry and dissolved oxygen dynamics in semi-enclosed bays. These findings provide important insights for the remediation of risks of hypoxia and harmful algal blooms in coastal mariculture ecosystems.

1. Introduction

The intersection of riverine and marine systems in the coastal zone creates a dynamic environment with unique conditions for organic matter dynamics (Chen, 2003). Organic matter in this area originates from allochthonous sources (e.g. terrestrial riverine input, marine sourced organic matter), autochthonous sources (such as phytoplankton production), and anthropogenic sources (e.g. sewage, fertilizer). Those organic matters can either bury and transform within coastal zones and/or exchange with oceanic seawater (Middelburg and Nieuwenhuize, 1998; Thomas et al., 2004; Lu et al., 2021) and thus play a significant role in elemental cycling, including carbon and nitrogen cycling, in coastal areas (Middelburg and Levin, 2009). Concurrently, coastal regions are of particular importance to human populations as they support most sea-based economic activities, despite their small area. These regions generate the majority of the sea-sourced food and resources that humans rely on (Martínez et al., 2007). The increasing population surges the demand for seafood, which has led to rapid expansions of coastal

* Corresponding authors at: Third Institute of Oceanography, Ministry of Natural Resources, Xiamen 361005, China.
E-mail addresses: hanaiqin@tio.org.cn (A. Han), linhui@tio.org.cn (H. Lin).

https://doi.org/10.1016/j.aquaculture.2023.740109
Received 6 May 2023; Received in revised form 7 September 2023; Accepted 14 September 2023
Available online 21 September 2023

mariculture in recent decades (Clawson et al., 2022). This expansion fuels the organic matter in coastal regions (as high as ~ 80%, (Hu et al., 2012; Dong et al., 2000), including fresh fish scrap, feeding fodder, and faeces (Pearson and Black, 2001; Vizzini and Mazzola, 2006), leading to the oxygen depletion/hypoxia through particulate organic matter (POM) degradation (Hargreaves, 1998; Vizzini and Mazzola, 2006; Yokoyama et al., 2006).

Remineralization of organic matter is a well-known driver for oxygen depletion or hypoxia in coastal regions (Swarzenski et al., 2008; Zhu et al., 2011). As such, there is a growing interest in understanding the dynamics of POM in the coastal zone. Semi-enclosed bays, which provide a haven for mariculture by offering protection from wave and wind damage, have a low degree of openness that increases the water residence time within the bay. This prolonged residence time consequently results in intensive recycling of POM and associated biogeochemical processes that have yet to be explored in detail.

Carbon and nitrogen isotopes have become increasingly popular in evaluating the sources and dynamics of POM (Riera and Richard, 1997; Vizzini et al., 2005; Yokoyama et al., 2006; Malet et al., 2008; Gu et al., 2017; Liu et al., 2018; Pan et al., 2019; Samanta et al., 2019; Xie et al., 2020a). For instance, some studies assessed the impact of anthropogenic input effect on POM in a coastal bay (Rožič et al., 2014; Samanta et al., 2019; Ke et al., 2020; Ming et al., 2023). Increasing studies qualitatively concerned the impact of anthropogenic loadings and resilience of the mariculture ecosystem (Franco-Nava et al., 2004; Sarà et al., 2004; Vizzini et al., 2005; Yokoyama et al., 2006; Malet et al., 2008). Past studies have employed isotopic mixing models to quantitatively evaluate the relative contributions of sources, but these have generally been applied only to sedimentary organic matter and have been restricted to two sources, with only a few studies examining multiple sources (Martinotti et al., 1997; Wu et al., 2003; Yokoyama et al., 2006; Liu and Kao, 2007; Dubois et al., 2012). Quantitative assessments of the relative contributions of multiple sources to an integrated mariculture ecosystem remain limited. Moreover, although both terrestrial and marine organic matter have been found contributing to oxygen consumption, such as marine organic matter degradation dominating hypoxia in the East China Sea off the Changjiang Estuary (Wang et al., 2016) and terrestrial organic matter accounting for 23% of oxygen depletion in the Gulf of Mexico (Dagg et al., 2007). The degradation of potential sources of settling POM associated with oxygen consumption in coastal mariculture bay ecosystem is not well understood (Malone and Newton, 2020; Hatakeyama et al., 2021). Lastly, the distinct behaviors of phytoplankton photosynthesis and POM remineralization revealed by ^{15}N associated with oxygen dynamics in biogeochemical stoichiometry have rarely been quantified (Sigman et al., 2009; Xu et al., 2022).

Coastal integrated mariculture bay ecosystems are highly complex, not only because they involved mixing processes from multiple sources (such as riverine input, coastal seawater transport, and mariculture activities), but also because they encompass biogeochemical processes across different water masses. Addressing these challenges requires a quantitative and holistic approach to accurately identify the contributions of different sources and to assess the potential degradation of organic matter associated with oxygen behavior.

To this end, we selected Sansha Bay, the largest breeding base of large yellow croaker (*Larimichthys crocea*) in China, as our study site. Sansha Bay is a semi-enclosed mariculture bay that is subject to influences from riverine inputs, nearshore seawater, and mariculture, making it a prime example of a coastal area that is applicable to similar bays around the world. This study, based on the field cruise, set out to examine the POM dynamics and potential degradation in such a complex physical and biogeochemical ecosystem. With the aid of three end-member water mass mixing and isotopic balance models, we are able to quantitatively evaluate POM origins and explore potential POM degradation associated with oxygen behavior. We find that in different regions with different POM sources and water residence time, the apparent degradation of POM associated dissolved oxygen dynamics and nitrogen cycling are different. The riverine POM dominates along the main channel under the influence of the water mixing, while autochthonous POM dominates in off-main channel region where water resident time is slow. In addition, POM degrades along the main channel to consume oxygen following the classic Redfield respiration stoichiometry. But regenerated dissolved inorganic nitrogen from feed food and riverine POM stimulate *in situ* phytoplankton production to complement oxygen following the canonical Redfield photosynthesis stoichiometry. This study pins down the relative contributions of different POM sources, as well as the potential effects of organic matter degradation and/or phytoplankton production on oxygen consumption and/or production and nitrogen cycling quantitatively using a combination of field observations and a simple three end-member mixing model in a complex semi-enclosed mariculture system under the influences of both river plume and coastal nearshore waters. The insightful POM dynamics associated with dissolved oxygen obtained in the semi-enclosed mariculture bay are important in defining the river-coastal continuum ecosystem and have important implications for a better understanding of the potential eutrophication, hypoxia, and harmful algal blooms in the mariculture ecosystems.

2. Materials and methods

2.1. Site description

Sansha Bay, situated in southeastern China, is a semi-enclosed bay with a highly meandering coastline (~489 km coastline, Fig. 1a) and is densely populated (~ 1000 people km^{-2} (Wang et al., 2009). The bay is connected to the East China Sea (ECS) via a narrow outlet known as Dongchong (DC) Channel (~3 km in width,) (Lin et al., 2017). The southwesterly winds prevail in summer, resulting in a northward predominance of the Taiwan Warm Current to Sansha Bay offshore (Hu et al., 2000). The monsoonal rainfall fuels the river flow in summer which potentially enhances the transportation of terrestrial materials into Sansha Bay (Li et al., 2009). The two primary freshwater sources discharging into Sansha Bay are Jiaoxi River and Huotongxi River. Jiaoxi Stream has a watershed of ~ 5549 km^2 with an average annual discharge of ~ 6.97×10^{10} m^3 (Huang and Ding, 2014). Huotongxi Stream has a watershed of ~2244 km^2 with an average annual discharge of ~ 2.73×10^9 m^3 (Li et al., 2014). The farmland surrounding Sansha Bay spans ~528 km^2 and the soil loss from the farmland into the bay has been estimated to be ~ 1.23×10^8 kg y^{-1} (Li et al., 2009). In recent decades, mariculture in Sansha Bay has significantly increased, with ~ 2.2×10^5 cages in the bay (Zhu et al., 2013). These cages are mainly located in the west of the bay, away from the north-south section from Baima Harbor to the DC channel, referred to as the off-main channel in Fig. 1. Moreover, inputs from feeding have been estimated to be as much as ~ 1.13×10^7 kg for fish fodder and ~ 7.55×10^8 kg for wet fresh fish scraps during the summer (Han et al., 2021).

2.2. Sampling and analysis

Summer cruises were conducted on August 6–8, 2014 to investigate the POM biogeochemistry. During the sampling period, the Jiaoxi water discharge from the watershed was ~ 365 m^3 s^{-1}, which was close to the long-term mean discharge (~ 175 m^3 s^{-1}) (Han et al., 2021). This suggests that the present study represents a typical summer condition of the area in terms of river discharge. Twenty-five water samples were collected using Niskin bottles equipped with a conductivity-temperature-depth (CTD, Idronaut S.r.l. Co., Italy) sensor that concurrently records temperature (T) and salinity (S). The sensors for T and S are Idronaut Pt 100 and Idronaut Seven rings. The precision for temperature and salinity are 0.003 °C and 0.005, respectively. Immediately after sampling, 500 mL of seawater was filtered onboard using pre-combusted (at 500 °C, for 4 h) and pre-weighted glass fibre filters (25 mm, Whatman GF/F). Following filtration, the filters with particulate

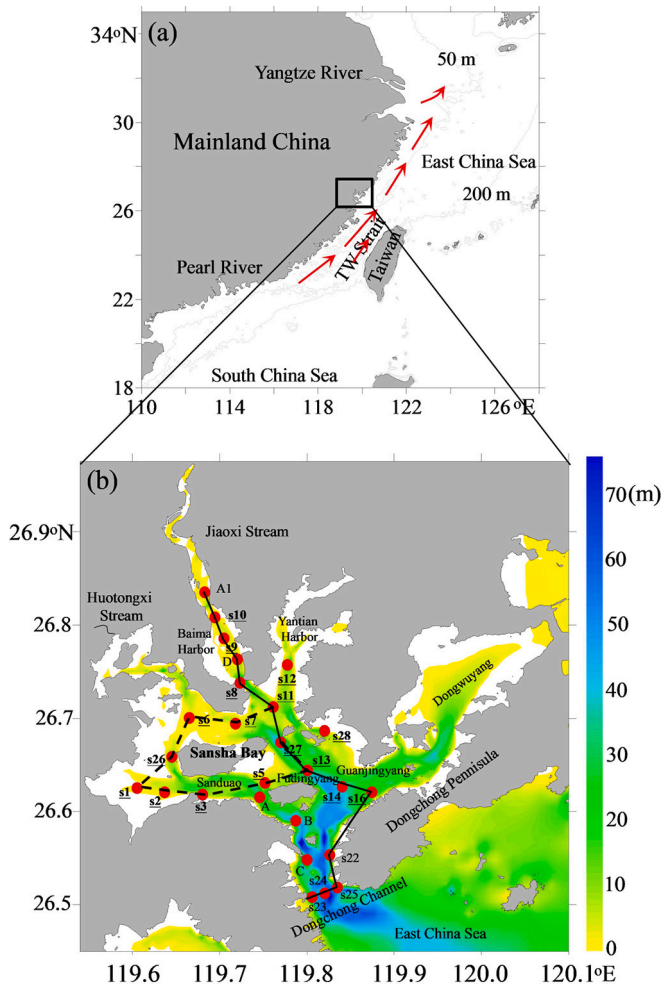

Fig. 1. Map of Sansha Bay indicating its location (a) and topography (in meters, b). The northward current under the prevailing southeast monsoon in summer is denoted by red arrows in (a). The main channel from Baima Harbor to Dongchong Channel is shown by the black line and the off-main channel is displayed by the black dashed line in (b). Water column sampling stations are marked by red dots, and surficial sediment sampling stations are indicated by black bottom lines. (For interpretation of the references to colour in this figure legend, the reader is referred to the web version of this article.)

samples were folded, wrapped in aluminum foil, and stored at −20 °C until laboratory analysis. Chlorophyll *a* (Chl *a*) concentration was determined using a Turner Trilogy fluorometer following the protocol of Welschmeyer (1994), with a detection limit 0.005 μg L^{-1}. The dissolved oxygen (DO) was measured using the traditional Winkler titration method with a precision of 1.88 μmol O_2 kg^{-1} (Dai et al., 2006). Apparent oxygen utilization (AOU) was as the difference between oxygen saturation (C_O^*) and DO, as $\ln C_O^* = -135.29996 + 1.572288 \times 10^5/(T + 273.15) - 6.637149 \times 10^7/(T + 273.15)^2 + 1.243678 \times 10^{10}/(T + 273.15)^3 - 8.621061 \times 10^{11}/(T + 273.15)^4 - S^*(0.020573 - 12.142/(T + 273.15) + 2363.1/(T + 273.15)^2)$ (Benson and Krause Jr., 1984)

In the laboratory, the filters were freeze-dried, and weighted for determining the concentration of total suspended particulate matter. The same filters were then used for analyzing particulate organic carbon (POC), particulate organic nitrogen (PN), $\delta^{13}C_{POC}$, and $\delta^{15}N_{PN}$. For analysis, the filters were acidified with 1 mL of 1 N HCl solution to remove carbonates, oven-dried at 60 °C for 48 h, and sliced for each parameter. A slice of filter (three-quarters size) was packed tightly into tin cans for POC and $\delta^{13}C_{POC}$ analysis and analyzed using a continuous flow elemental analyzer (Vario PYRO cube, Germany)-isotope ratio mass spectrometer (Isoprime 100) system (EA-IRMS). For PN and $\delta^{15}N_{PN}$ measurement, a slice of filter (quarter size) was oxidized to nitrate using potassium persulfate (Knapp et al., 2005) and nitrate was measured using the chemiluminescence method following the protocol of Braman and Hendrix (Braman and Hendrix, 1989). The detection limit of NO_X^- was ~ 10 nmol L^{-1}, and the precision was better than 5% (Xu et al., 2017). Samples were then analyzed using a Gas Bench-Isotope Ratio Mass Spectrometer GB-IRMS (Thermo Delta V Advantage, Germany) through the denitrifier method outlined in Xu et al. (2017). The isotopic compositions of carbon ($\delta^{13}C$) and nitrogen ($\delta^{15}N$) were expressed as follows:

$$\delta^{13}C \text{ or } \delta^{15}N = \left[\frac{R_{sample}}{R_{standard}} - 1\right] \times 1000$$

where R corresponds to $^{13}C/^{12}C$ or $^{15}N/^{14}N$ for carbon and nitrogen respectively. The standard reference materials were the international standards Pee Dee Belemnite for C and atmospheric N_2 for N, respectively. The replications of $\delta^{13}C_{POC}$ and $\delta^{15}N_{PN}$ for internal standards were better than 0.2‰ (Yang et al., 2017).

The N isotope of nitrate ($\delta^{15}N_{NO3}$) was determined using the bacterial denitrifier method (Sigman et al., 2001). Briefly, the NO_3^- in the water was converted to N_2O by denitrifying bacteria that lack N_2O reductase activity. Then, the N_2O was extracted and purified through a PreCon system (Thermo Fisher, USA), and the $\delta^{15}N$ was analyzed using an isotope ratio mass spectrometer (IRMS, USA). The $\delta^{15}N_{NH4}$ was determined using the chemical procedure (Zhang et al., 2007). Briefly, NH_4^+ in the water was first quantitatively oxidized to NO_2^- by BrO^- and subsequently NO_2^- is reduced to N_2O using NaN_3 in an acetic acid buffer. Then the $\delta^{15}N$ of N_2O was determined by PreCon-IRMS (USA). The NH_4^+ concentration for $\delta^{15}N$ measurement required relatively higher level, being >5.0 μmol L^{-1}. The standard deviations precisions for both $\delta^{15}N_{NO3}$ and $\delta^{15}N_{NH4}$ were better than 0.5‰.

Surficial sedimentary samples (the top 1.0 cm) in the off-main channel were collected (Fig. 1), while sample collection in the main channel was not possible due to the fast flow and rough granular composition. Surficial sediment samples were immediately collected with a Van Veen grab sampler, frozen, and stored at −20 °C. Samples of fish feed fodder and fresh fish scraps were freeze-dried, and the POC and PN contents associated with dual-isotopic compositions were measured using an elemental analyzer connected with isotope ratio mass spectrometry (EA-IRMS, Elementary Vario PYRO cube, Germany). The precisions for POC and PN content were < 1% and dual-isotopic compositions were better than 0.2‰ for standard measurement (Kao et al., 2012; Yang et al., 2017).

2.3. Derivation of three end-member isotopic mixing model

A three end-member isotopic mixing model is used to construct the conservative mixing schemes among different particle sources in the entire mariculture ecosystem. The $\delta^{13}C_{POC}$ values and C/N ratios in particles generally enhance the source apportionment and therefore have been established. A detailed derivation of the multiple end-member isotopic mixing model had been introduced in previous research (Liu and Kao, 2007; Liu and Wu, 2014). In brief, the model is based on mass balance for POC and PN, and for the isotope $\delta^{13}C_{POC}$ in POC, which originate from the three sources introduced in following Sections 3 and 4. The equations are shown as follows:

$$R_{in\ situ} = F_{RI}R_{RI} + F_{DC}R_{DC} + F_{BIO}R_{BIO} \quad (1)$$

$$\delta^{13}C_{POCin\ situ} = F_{RI}\delta^{13}C_{POCRI} + F_{DC}\delta^{13}C_{POCDC} + F_{BIO}\delta^{13}C_{POCBIO} \quad (2)$$

$$F = F_{RI} + F_{DC} + F_{BIO} \quad (3)$$

where $R_{in\ situ}$ and $\delta^{13}C_{POCin\ situ}$ represented the C/N ratio and $\delta^{13}C_{POC}$ in the samples; the subscripts RI, DC, and BIO denoted the three different particle end-members: riverine POM from upstream river plume (RI),

riverine POM occupied in coastal nearshore water (DC), and autochthonous phytoplankton (BIO); and F_{RI}, F_{DC}, and F_{BIO} represent the fractions in the *in situ* particle samples contributed by the three end-members, which are calculated from the C/N ratio and $\delta^{13}C_{POC}$.

The conservative isotopic nitrogen composition of PN ($\delta^{15}N_{PNpre}$) by mixing of the end-members can then be calculated as.

$$\delta^{15}N_{PNpre} = F_{RI}\delta^{15}N_{PNRI} + F_{DC}\delta^{15}N_{PNDC} + F_{BIO}\delta^{15}N_{PNBIO} \quad (4)$$

where $\delta^{15}N_{PNRI}$, $\delta^{15}N_{PNDC}$, and $\delta^{15}N_{PNBIO}$ are the isotopic nitrogen compositions of the three end-members of river plume, coastal seawater, and the *in situ* phytoplankton production.

The difference between the prediction based on mass balance and the field measured values is denoted as Δ, which helps to reveal the nitrogen biogeochemical cycles and associated oxygen dynamics.

$$\Delta\delta^{15}N_{PN} = \delta^{15}N_{PNpre} - \delta^{15}N_{PN\,in\ situ} \quad (5)$$

where $\delta^{15}N_{PN\,in\ situ}$ represents the measured isotopic nitrogen composition of PN during the cruise.

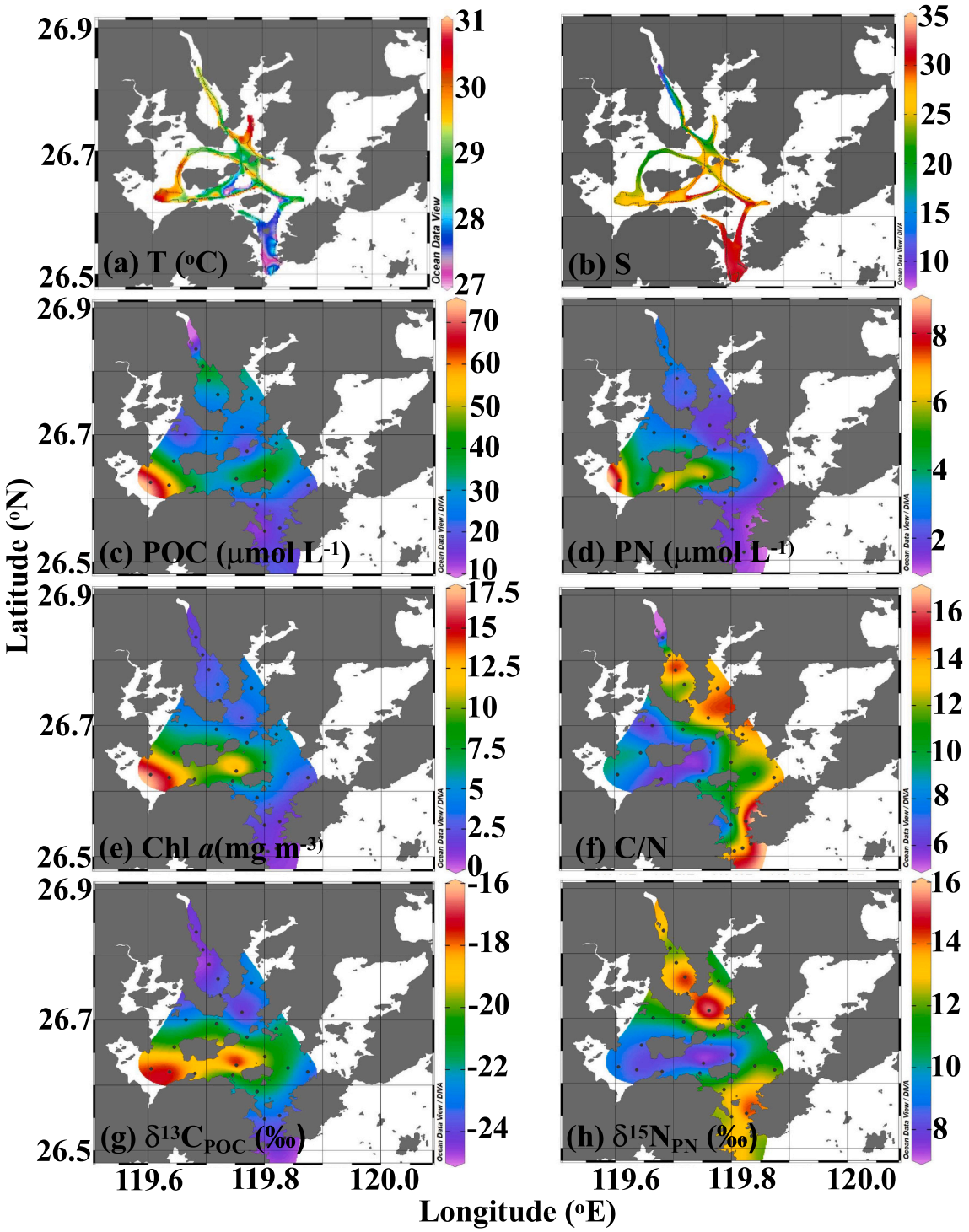

Fig. 2. Surface distributions of temperature (a, °C), salinity (b, S), particulate organic carbon (c, μmol L^{-1}), particulate organic nitrogen (d, μmol L^{-1}), Chl *a* (e, mg m^{-3}), C/N ratio (f), $\delta^{13}C_{POC}$ (g), and $\delta^{15}N_{PN}$ (h) in Sansha Bay. The temperature and salinity distributions are redrawn from Han et al., 2021).

2.4. Definitions of ΔDIN, ΔDIP, and ΔPN

Similar to $\Delta\delta^{15}N_{PN}$, ΔDIN, ΔDIP, and ΔPN represent the differences between the predicted dissolved inorganic nitrogen (nitrate (NO_3^-) + nitrite (NO_2^-) + ammonia (NH_4^+), DIN), dissolved inorganic phosphorus (DIP), and PN based on conservative mixing and the field measured values, respectively, and are calculated based on three end-member water mass mixing model (Han et al., 2021). The positive ΔDIN and ΔDIP indicate nutrient consumed by phytoplankton and negative values indicate nutrient addition via organic matter degradation. Similarly, positive and negative ΔPN represent PN removal and production, respectively. In our parallel studies, ΔDIN and ΔDIP properties have been elaborated by Han et al. (2021). Here, we introduce ΔDIN, ΔDIP, and ΔPN equations in Text S1 briefly.

3. Results

3.1. Hydrography

The hydrography observed during the cruise in Sansha Bay has been documented by Han et al. (2021). The warm river plume with a temperature of ~ 29.2–29.6 °C and salinity of ~ 9.6–20.8 spreads southward through Baima Harbor, mixing with coastal seawater with a temperature of ~ 28.1–27.2 °C and salinity of ~ 29.6–31.2 over semi-diurnal tidal cycles. As a result, the study area is mainly characterized by a mixed water mass along the main channel with temperature ~ 29.3–27.2 °C and salinity ~ 20.8–31.2 (Fig. 2a, b). The off-main channel has relatively enclosed water with high temperature (29.4–30.8 °C) and mid-salinity (22.7–26.7, Fig. 2a, b) due to the bathymetry, resulting in a longer water residence time (Lin et al., 2017). Therefore, the study area can be divided into two hydrographic zones: the north-south section along the main channel, primarily showing mixing between riverine and coastal waters, and the west side of the bay (i.e., off-main channel).

Further examination of the temperature and salinity sections along the north-south section illustrates the extension of the river plume with clear stratification, where the saltier coastal water intrudes below the fresh riverine water (Figs. 3a, b, 4a, b). The intrusion intensity of the coastal water via DC channel is strong in the mid-bay, i.e., south of S27 along the main channel and south of S1 and S5 along the off-main channel, as indicated by the lower temperature (~ 26.3–28.3 °C) and higher salinities (~ 26.9–32.6).

3.2. Distribution of biogeochemical parameters

3.2.1. Spatial distribution of parameters at surface waters

The horizontal distributions of POC and PN show a clear zonation in the main channel and western off-main channel, consistent with the hydrographic conditions. The upstream stations in the main channel (Figs. 1 and 2), influenced by the river plume, exhibit relatively higher POC (~ 16.4–43.0 μmol L^{-1}) and lower PN (~ 2.1–3.2 μmol L^{-1}), which

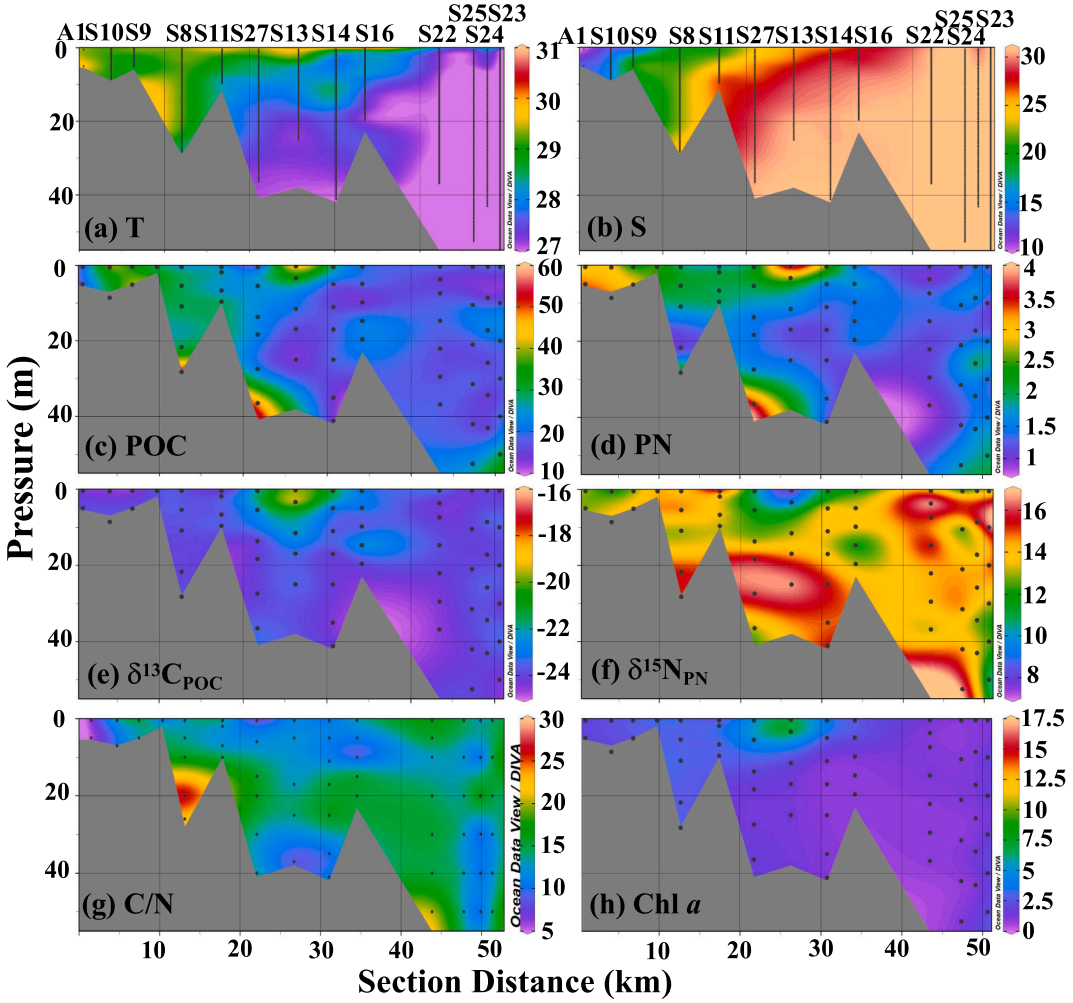

Fig. 3. Transectional distribution of T (a, °C), S (b), POC (c, μmol L^{-1}), PN (d, μmol L^{-1}), C/N ratio (e), Chl *a* (f, mg m^{-3}), $\delta^{13}C_{POC}$ (g), and $\delta^{15}N_{PN}$ (h), along the north-south main channel in Sansha Bay. The temperature, salinity, and Chl *a* are redrawn from Fig. 7a, b and Fig. 12d in Han et al., 2021). Black dots represent the sampling depth.

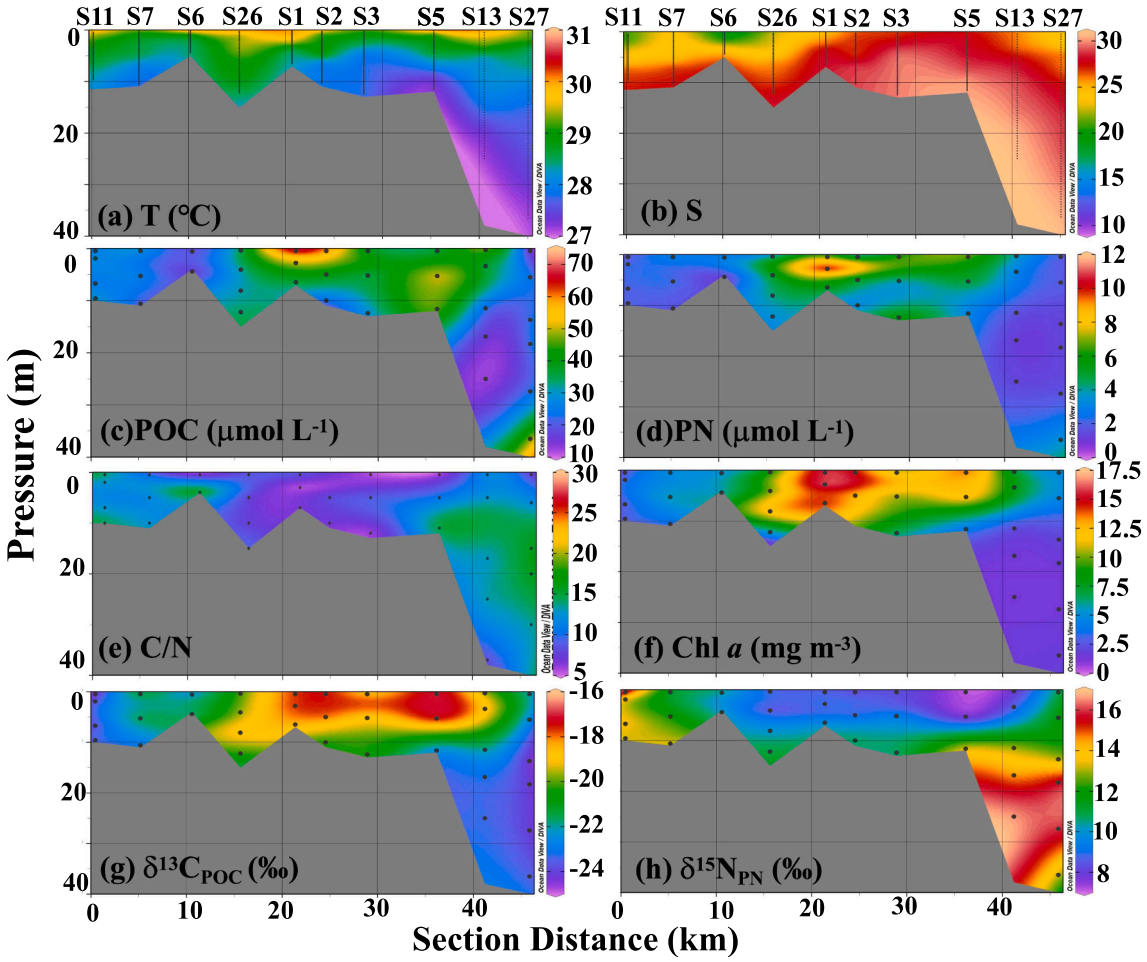

Fig. 4. Transectional distribution of T (a, °C), S (b), POC (c, μmol L^{-1}), PN (d, μmol L^{-1}), C/N ratio (e), Chl *a* (f, mg m^{-3}), $\delta^{13}C_{POC}$ (g), and $\delta^{15}N_{PN}$ (h) along the western off-main channel in Sansha Bay. Black dots represent the sampling depth.

coincides with higher nutrient concentrations in the dissolved pool (DIN, ~ 41.8–47.1 μmol L^{-1}), *see* Fig. 5 in Han et al., 2021). The downstream stations are influenced by coastal water, showing lower POC (~ 16.5–19.7 μmol L^{-1}) and lower PN (~ 1.1–1.6 μmol L^{-1}), consistent with low dissolved nutrient levels mainly due to dilution by coastal seawater (Naik and Chen, 2008; Han et al., 2021). In mid-Sansha Bay, which geographically corresponds to the area between the upstream and downstream stations, the POC and PN concentrations show intermediate values of ~16.5–26.1 μmol L^{-1} and ~ 1.1–2.6 μmol L^{-1}, respectively, along with lower nutrient levels in the dissolved pool (~ 16.1–34.3 μmol L^{-1} DIN). The particulate C/N ratios along the north-south section range from ~ 10.2 to ~ 16.5 (Fig. 2f).

In the western off-main channel, the POC and PN contents are extremely high, ranging from ~ 25.9–71.3 μmol L^{-1} for POC and ~ 2.5–8.3 μmol L^{-1} for PN. This location also exhibits the highest Chl *a* (~ 10.4–16.6 mg m^{-3}), the lowest DIN concentration (~ 11.2–12.7 μmol L^{-1}, *see* Fig. 5 in Han et al., 2021), and the highest DIN uptake concentration (~ 2.0–10.5 μmol L^{-1}) (Figs. 2c, d, e, and S1). These findings suggest strong nutrient consumption and high phytoplankton biomass in the western off-main channel, which has a longer water residence time than the main channel (Lin et al., 2017). The C/N ratios in the western side of the bay range between ~ 5.8–9.0 (Fig. 2f).

The spatial distributions of POM isotopic compositions ($\delta^{13}C_{POC}$ and $\delta^{15}N_{PN}$) display clear zonation similar to POC, PN, and the water masses (Fig. 2a, b, g, h). The surface $\delta^{13}C_{POC}$ values in Sansha Bay range from −24.7‰ to −17.2‰, and the $\delta^{15}N_{PN}$ range from 7.8‰-15.9‰. Along the north-south section, the $\delta^{13}C_{POC}$ and $\delta^{15}N_{PN}$ vary from −24.7‰ to −21.4‰ and 11.8‰ to 14.9‰, respectively, with the lighter $\delta^{13}C_{POC}$ (< −23.6‰) and heavier $\delta^{15}N_{PN}$ (~ 14.9‰) located upstream near the Baima Harbor. Downstream from Baima harbor and around the DC channel, both $\delta^{13}C_{POC}$ and $\delta^{15}N_{PN}$ show narrow ranges, specifically ~ −23.2‰–24.5‰ for $\delta^{13}C_{POC}$ and ~ 12.2‰-14.5‰ for $\delta^{15}N_{PN}$. In the western off-main channel, heavy $\delta^{13}C_{POC}$ and light $\delta^{15}N_{PN}$ are observed, with ranges of ~ −21.3‰- -17.2‰ for $\delta^{13}C_{POC}$ and ~ 7.2‰-9.0‰ for $\delta^{15}N_{PN}$. Concurrently, the region exhibiting the lightest $\delta^{15}N_{PN}$ values coincides with the heaviest $\delta^{13}C_{POC}$ (~ −19‰–17‰), the highest POM concentrations (POC, ~ 25–70 μmol L^{-1} and PN ~ 4–8 μmol L^{-1}), and the greatest DIN uptake concentration (~ 2.5–12.5 μmol L^{-1}) (Figs. 2c, d, g, h, S1). These observations strongly support that *in situ* phytoplankton production dominates the POC in the west region of the bay.

3.2.2. *Longitudinal distribution of parameters*

Figs. 3 and 4 illustrate the hydrographical and biogeochemical parameters of POM across the north-south main channel and the western off-main channel, respectively. Along the main channel, POC and PN distributions closely follow the water mass mixing. The POC and PN concentrations peak at the river plume wedge and decrease rapidly towards the mid-bay region, ranging from ~ 43.0 μmol L^{-1} to ~ 24.9 μmol L^{-1} and from ~ 4.0 μmol L^{-1} to ~ 1.1 μmol L^{-1}, respectively. We observed extremely high POC and PN at station S13, with values of ~ 45.0 μmol L^{-1} for POC and ~ 3.5 μmol L^{-1} for PN, along with the highest Chl *a* of ~ 7.5 mg m^{-3}. Beneath the river plume, POC, PN, and Chl *a* levels decrease following the water mass mixing (POC ~ 10.0–20.0 μmol L^{-1}, PN ~ 0.9–1.5 μmol L^{-1}, and Chl *a* ~ 1.0–1.5 mg m^{-3}, respectively). The C/N ratio along the main channel range between ~ 5.4 and 16.0, with an average of ~ 12.7 (Fig. 3c, d, g, h). In contrast to

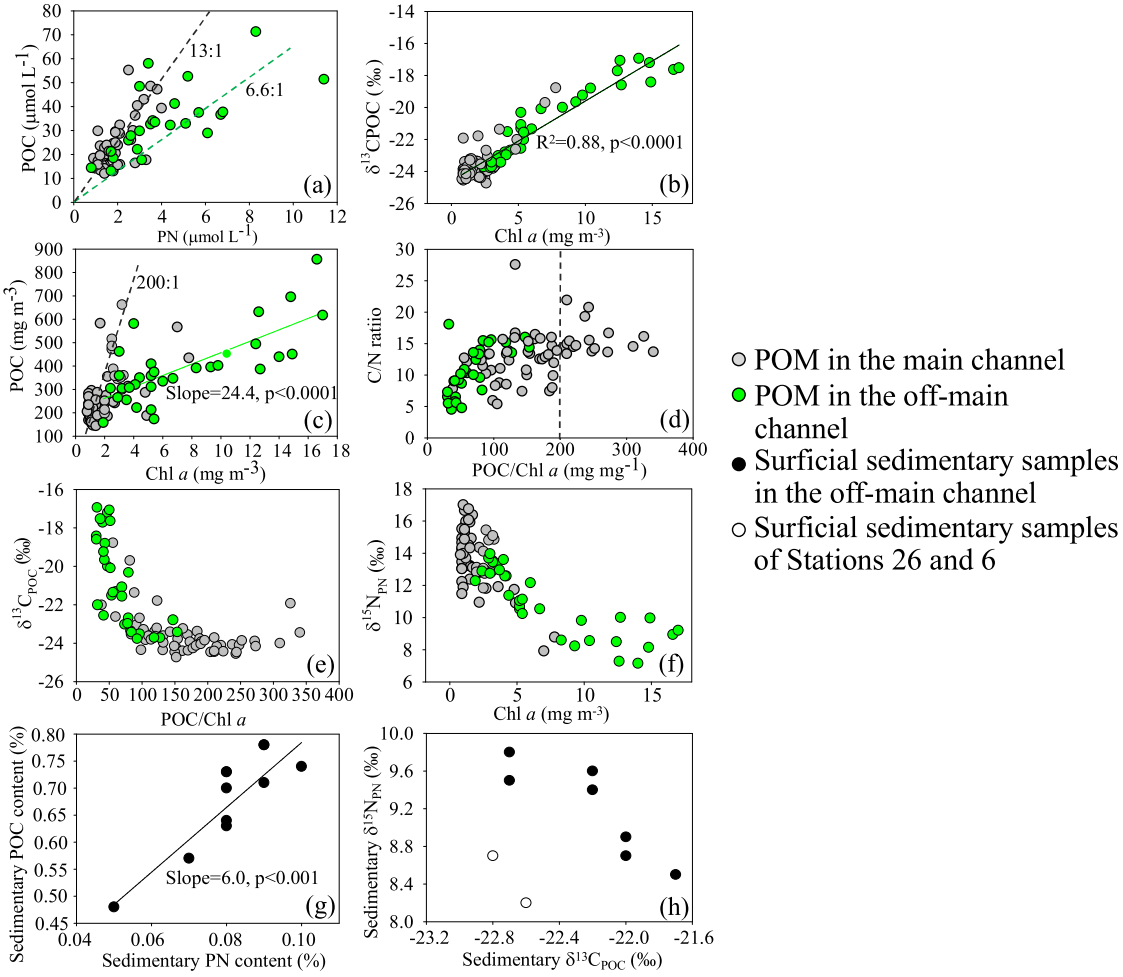

Fig. 5. Linear correlation analyses of various parameters in Sansha Bay, including (a) POC vs. PN, (b) $\delta^{13}C_{POC}$ vs. Chl *a*, (c) POC vs. Chl *a*, (d) C/N ratio vs. POC/Chl *a*, (e) $\delta^{13}C_{POC}$ vs. POC/Chl *a*, (f) $\delta^{15}N_{PN}$ vs. Chl *a*. In (g), the surficial sedimentary POC vs. PN and (h) surficial sedimentary $\delta^{15}N_{PN}$ vs. $\delta^{13}C_{POC}$ in the western off-main channel are shown. Gray dots in (a-f) indicate samples collected in the main channel, while green dots indicate samples collected in the off-main channel. Black dots represent surficial sedimentary samples in the off-main channel, and blank dots represent surficial sedimentary samples of Stations 26 and 6. The black and green dashed lines in (a) represent the C/N ratio of averaged farmland soil (~ 13) and Redfield C/N ritao (~ 6.6), respectively. The solid line in (b) represents the correlation in the entire Sansha Bay. The dashed line in (c) and (d) represents the POC/Chl *a* ratio value of 200 mg mg^{-1}, a threshold used to define the dominance of phytoplankton in the POM (Liu et al., 2018). The green solid line in (c) indicates the POC/Chl *a* ratio of 24.4 mg mg^{-1} in the off-main channel. The solid line in (g) indicates the C/N ratio of surficial sedimentary samples. (For interpretation of the references to colour in this figure legend, the reader is referred to the web version of this article.)

the physico-chemical gradient of POM observed, the $\delta^{13}C_{POC}$ and $\delta^{15}N_{PN}$ distributions along the main channel are relatively homogeneous across the water column, with values of $\delta^{13}C_{POC}$ ~ −24‰ and $\delta^{15}N_{PN}$ ~ 14‰-16‰, except at S13 ($\delta^{13}C_{POC}$ ~ −18.8‰- -19.7‰ and $\delta^{15}N_{PN}$ ~ 14–16‰) where high Chl *a* has been observed (Fig. 3e, f, h).

The western off-main channel exhibits lower impacts from the river plume, as indicated in Fig. 4. The POC and PN contents in this region reach levels as high as ~ 33.5–71.3 μmol L^{-1} and ~ 3.7–11.4 μmol L^{-1}, respectively. The C/N ratios show relatively stable range of ~ 4.5–10.2 (with an average of ~ 9.3) while the Chl *a* reaches extremely high levels (as high as ~ 5–16 mg m^{-3}), suggesting that the west off-main channel is stimulated by strong DIN consumption (Fig. S1). Correspondingly, heavier $\delta^{13}C_{POC}$ (~ −17‰ - -19.5‰) and lighter $\delta^{15}N_{PN}$ (~ 7.5‰ - 9.5‰) are widespread throughout the entire western bay.

4. Discussion

4.1. Distinct riverine and autochthonous POM revealed by C/N ratio, $\delta^{13}C_{POC}$, and $\delta^{15}N_{PN}$

Isotopic compositions and molar elemental ratios of organic matter are useful for analyzing POM sources (Meyers, 1994; Savoye et al., 2003; Liu and Kao, 2007; Liu et al., 2018). POM from riverine allochthonous and autochthonous sources can be distinguished by their C/N ratios and $\delta^{13}C_{POC}$ values. Riverine allochthonous POM typically has a higher C/N ratio (>12) (Hedges and Man, 1979; Gordon and Goñi, 2003; Wu et al., 2003) and lighter $\delta^{13}C_{POC}$ (−18‰ to −24‰ in Gearing et al., 1984; Wada et al., 1987; −19‰- -15‰ in Fry and Wainright, 1991; −22‰- -18‰ in Cifuentes et al., 1996; −26‰ in Kao et al., 2003; −16‰- -20‰ in Savoye et al., 2003; −24‰ - -22‰ in Liu et al., 2018), while

Table 1
Carbon and nitrogen content and dual isotopic compositions of the surficial sediment and feed food in Sansha Bay.

Sample	POC content (%)	Mean ± SE (%)	$\delta^{13}C_{POC}$ (‰)	Mean ± SE (‰)	PN content (%)	Mean ± SE (%)	$\delta^{15}N_{PN}$ (‰)	Mean ± SE (‰)	C/N ratio
S1	0.71		−22.2		0.09		9.4		8.9
S2	0.63		−22.2		0.08		9.6		9.4
S5	0.64		−22.0		0.08		8.9		9.0
S6	0.73		−22.6		0.08		8.2		10.2
S7	0.48	0.68 ± 0.10	−22.7	−21.5 ± 0.9	0.05	0.08 ± 0.01	9.8	9.1 ± 0.6	10.7
S11	0.70		−22.7		0.08		9.5		10.1
S14	0.82		−13.7		0.07		10.0		12.9
S16	0.57		−22.0		0.07		8.7		9.4
S26	0.78		−22.8		0.09		8.7		10.0
S28	0.74		−21.7		0.10		8.5		9.0
	43.01		−15.4		10.45		11.6		4.8
Fresh fish scrap	39.36	42.53 ± 2.95	−15.1	−15.3 ± 0.2	9.75	10.39 ± 0.61	11.5	11.6 ± 0.1	4.7
	45.21		−15.5		10.97		11.7		4.8
	43.82		−23.8		6.73		6.2		7.6
Fish feed fodder	43.44	43.51 ± 0.28	−22.7	−23.4 ± 0.6	6.94	6.81 ± 0.12	5.9	6.0 ± 0.2	7.3
	43.27		−23.7		6.76		5.9		7.5

autochthonous POM has lower C/N ratio (~ 6–9 in Holligan et al., 1984; Wu et al., 2003; 4–10 in Dan et al., 2019) and heavier $\delta^{13}C_{POC}$ values (−22‰ - -19‰) (Goericke and Fry, 1994; Meyers, 1994; Kao et al., 2003; Liu et al., 2018).

The POC and PN in the entire Sansha Bay show a strong linear relationship ($R^2 = 0.67$, $p < 0.0001$), and most C/N ratios in POM fall within the range of riverine farmland soil C/N ratio (~ 13 in Ma and Wang, 2011; Jiang et al., 2017; ~ 10.1 in Xie et al., 2020b; ~ 11.7 in Hu et al., 2022) and classic Redfield C/N ratio of autochthonous POM (~ 6.6 in Redfield et al., 1963) (Fig. 5a), suggesting that particles in the entire Sansha Bay ecosystem likely resulted from riverine allochthonous origins transported upstream river plume combined with *in situ* phytoplankton production. High phytoplankton productivity can decrease carbon fractionation and enrich $\delta^{13}C_{POC}$ value in POM (Liu et al., 2018, and references therein), resulting in a strong positive correlation between $\delta^{13}C_{POC}$ and Chl *a* in Sansha bay ($R^2 = 0.88$, $p < 0.0001$, Fig. 5b). Fig. 5c also indicated that phytoplankton is dominant in the western POC pool with a positive POC vs. Chl *a* relationship ($R^2 = 0.55$, $p < 0.0001$) but not in the main channel. In general, the POC/Chl *a* ratio can also be used to differentiate between POM sources in coastal waters (Cifuentes et al., 1988). The derived POC/Chl *a* in the western bay was 24.4 mg mg^{-1}, close to the prior POC/Chl *a* ratio in East China Sea, indicating *in situ* phytoplankton production featured by heavy $\delta^{13}C_{POC}$ (i.e., 34.1–36.1 mg mg^{-1}, Cifuentes et al., 1996; Chang et al., 2003; Savoye et al., 2003; Liénart et al., 2016; Liu et al., 2018) (Fig. 5c, d). Since POC/Chl *a* ratio higher than 200 mg mg^{-1} is attributable to detrital or degraded organic matter (heterotrophic/mixture-dominated) (Cifuentes et al., 1996; Savoye et al., 2003; Liénart et al., 2016; Liu et al., 2018), POM in the main channel is primarily contributed by riverine POM, characterized by high POC/Chl *a* (~100–350 mg mg^{-1}), together with light $\delta^{13}C_{POC}$ (~ −22‰- -24.5‰), high C/N ratios, and wide $\delta^{15}N_{PN}$ values (~11‰-17‰), resulting from multiple allochthonous and anthropogenic mixture POM from upstream Jiaoxi River (Fig. 2h, 5b, d, e). The slightly scattering in the observed POM between 24.4 mg mg^{-1}-200 mg mg^{-1} is probably co-influenced by autochthones POM in the off-main channel and riverine POM in the main channel via water mass mixing.

Furthermore, in the off-main channel (Fig. 1, Table 1), the correlation between POC and PN contents in the surficial sediments is strong ($y = 6.0\times + 0.0018$, $R^2 = 0.81$, $p < 0.0001$) and the C/N ratio is closed to

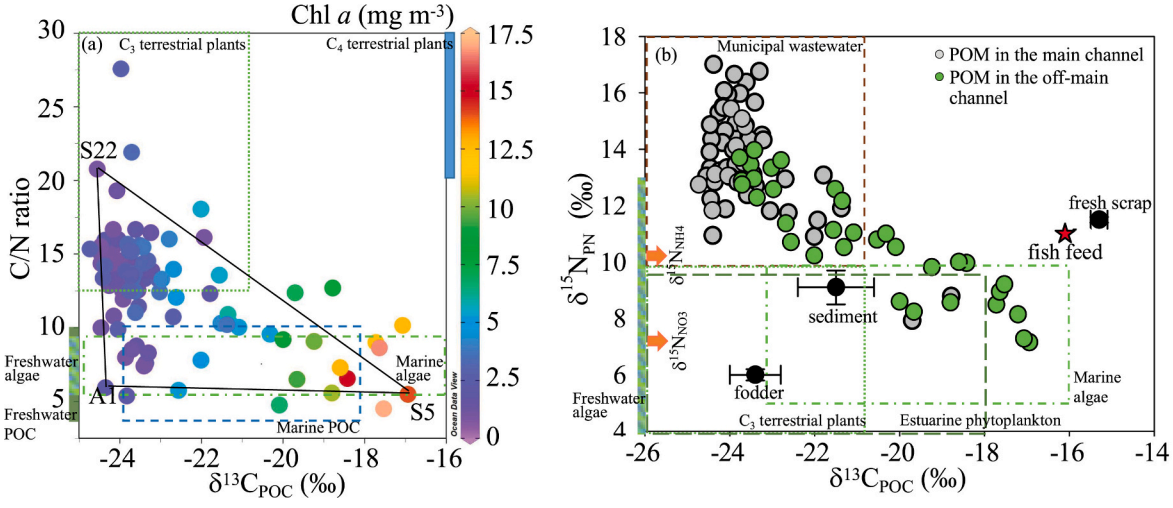

Fig. 6. (a) Bi-plot of $\delta^{13}C_{POC}$ and C/N ratio of POM in Sansha Bay, overlapped with Chl *a* concentration (mg m^{-3}). Typical $\delta^{13}C_{POC}$ and C/N ratio ranges for three different organic matter end-members in the entire bay were also indicated with a triangle. (b) Bi-plot of $\delta^{13}C_{POC}$ and $\delta^{15}N_{PN}$ features of POM and other specified particles (fodder, fresh scrap, and surficial sediment) in Sansha Bay. Gray dots in (b) indicate samples collected in the main channel, and green dots indicate samples collected in the off-main channel. Red star in (b) represents the estimated isotopic composition ($\delta^{13}C_{POC}$ and $\delta^{15}N_{PN}$) of fish feed based on ~ 90% fresh fish scrap and ~ 10% fodder. Typical C/N ratio, $\delta^{13}C_{POC}$, and $\delta^{15}N_{PN}$ ranges for different organic matter end-members were also plotted in (a) and (b) drawn by dashed rectangles, referring from Lamb et al. (2006), Gao et al. (2021), and references therein. Orange arrows indicate values of $\delta^{15}N_{NO3}$ and $\delta^{15}N_{NH4}$. (For interpretation of the references to colour in this figure legend, the reader is referred to the web version of this article.)

Table 2
Defined end-member properties used in the model described in Section 4.2.2 along with their reference values and the error propagation (ε_F) assessment associated the fraction source values in the three end-member isotopic mixing model. See Eq. (6) for the error propagation calculation.

End-members	Observed $\delta^{13}C_{POC}$ (‰)	Adopted $\delta^{13}C_{POC}$ (‰)	Observed C/N ratio	Adopted C/N ratio[#]	ε_F (%)
River plume[#]	−24.09 ± 0.36	−24.35	5.66 ± 0.40	5.94	4
Coastal nearshore water[#]	−24.11 ± 0.46	−24.57	15.81 ± 2.46	18.27	3
in situ phytoplankton production[*]	~ − 16- -24.5	−16.94	~5–9	5.49	1

[*] : Station S5 is selected as the *in situ* phytoplankton production end-member (−16.94‰ for $\delta^{13}C_{POC}$, and 5.49 for C/N ratio, Fig. 6a), based on its particle isotopic composition which exhibits a close agreement with reported observed values (Gao et al., 2021, and references therein), and also satisfied the criteria for end-member selection according to Kao and Liu (2007).
[#] :A1 is identified as the river plume end-member, while S22 is identified as the coastal nearshore water end-member.

Redfield ratio (6.6:1) (Fig. 5g). The $\delta^{13}C_{POC}$ and $\delta^{15}N_{PN}$ isotopic compositions show a narrow range (as −21.7‰- -22.8‰ for $\delta^{13}C_{POC}$ and 8.5‰-9.8‰ for $\delta^{15}N_{PN}$), falling between the dual isotopic ranges of riverine POM in the main channel water column and *in situ* autochthonous POM in western bay water, and isotopically closer to the latter (Fig. 5h). These findings suggest that autochthonous POM dominates sedimentary organic matter in the western bay, while co-influenced by riverine POM transported via water mass mixing, which settles on the seafloor and becomes part of the sedimentary organic matter in the western bay.

In summary, our results indicate that the POM in the entire Sansha Bay ecosystem mixes among the riverine transported POM in the main channel and in situ phytoplankton production in the off-main channel with minor influence with the water mixing.

4.2. Sources apportionment of POM

4.2.1. Selection of three POM end-members

In aquatic ecosystem, C/N ratios and elemental isotopic compositions are utilized not only to identify the origin of materials (Andrews et al., 1998; Middelburg and Nieuwenhuize, 1998) but also commonly used to assess the mixing of various POM sources (Shultz and Calder, 1976; Kao et al., 2006; Liu and Kao, 2007; Yu et al., 2015).

The $\delta^{13}C_{POC}$ along the main channel displays a riverine-coastal trend with narrow and light $\delta^{13}C_{POC}$ values (~ −24- -22‰). However, the plots of wide C/N ratio (~ 5–20) and $\delta^{13}C_{POC}$ overlaid with low Chl *a* (< ~ 4.5 mg m^{-3}) along the main channel indicate the presence of riverine (and/or freshwater influenced) POM end-members (i. e., the riverine stations A1 and S10 in Baima Harbor) and riverine POM around the DC channel (i.e., station S22) (Figs. 1 and 6a). On the other hand, plots of C/N ratio (~ 4.5–12.7) and wide $\delta^{13}C_{POC}$ (−20.0‰–16.9‰) with high Chl *a* (> ~ 4.5 mg m^{-3}) in the western bay indicate the dominance of autochthonous POM/algae, significantly influenced by riverine POM via water circulation, showing strong signals associated with maricultural activities. The representative end-member station S5 in the western off-main channel, is characterized by high Chl *a* (~13 mg m^{-3}), the heaviest $\delta^{13}C_{POC}$ (~ −16.8‰), and low C/N ratio (~ 5) (Fig. 6a). Most of the remaining POM in Sansha Bay scatters within the domain bounded between downstream river plume, nearshore DC channel, and western bay (Fig. 6a). Thus, the scatter distributions of C/N ratios vs. $\delta^{13}C_{POC}$ indicated three distinct particle end-members mixing within Sansha Bay, namely riverine POM extending from the upstream river plume to the nearshore DC channel and autochthonous phytoplankton occupying the western off-main channel (Han et al., 2021; Lin et al., 2017).

Although the salinity gradient indicates an obvious intrusion of coastal seawater through tidal mixing, the duel isotopic compositions of particle end-members from the upstream river plume to the coastal DC channel, namely the $\delta^{13}C_{POC}$ and $\delta^{15}N_{PN}$, were indistinguishable, with narrow ranges of −24.5‰–23.5‰ for light $\delta^{13}C_{POC}$ and 11‰-17‰ for heavy $\delta^{15}N_{PN}$, which likely due to strong water mass mixing along the main channel, as shown in Fig. 6b. Thus, it is not feasible to accurately identify the end-members via the relationship between $\delta^{13}C_{POC}$ and $\delta^{15}N_{PN}$. Particles in the off-main channel were characterized by heavy $\delta^{13}C_{POC}$ and light $\delta^{15}N_{PN}$ (i.e., ~ −17‰–20‰ for $\delta^{13}C_{POC}$, ~ 7‰-10‰ for $\delta^{15}N_{PN}$), which clearly indicates the dominance of flourishing phytoplankton, as previously introduced. Additionally, the general decreasing $\delta^{13}C_{POC}$ and increasing $\delta^{15}N_{PN}$ towards the main channel indicate hydrological connectivity within Sansha Bay, consistent with other parameters (T, S, and nutrients).

Following the three end-members set (Liu and Kao, 2007), i.e., firstly, each of the three end-member compositions should fall within one standard deviation of the observed or derived mean values of materials originating from the source; secondly, most of the observed compositions of mixtures should fall within the domain defined by the three members or very close to the domain, and according to the scatter plots between $\delta^{13}C_{POC}$ and C/N ratio (Fig. 6a), the properties of the end-members are adopted from observed this study or derived values. Particles from riverine input with C/N ratio ~ 5.94 and $\delta^{13}C_{POC}$ ~ −24.35‰ served as the river plume end-member, and particles around DC channel with C/N ratio ~ 18.27 and $\delta^{13}C_{POC}$ ~ −24.57‰ are defined as the coastal seawater end-member. We also define the particle isotopic composition with C/N ratio ~ 5.49 and $\delta^{13}C_{POC}$ ~ −16.94‰ occupied the western off-main channel as the end-member for phytoplankton production. The model parameters are presented in Table 2.

The propagated error of the fraction estimation due to the selection of end-member properties has been tested. From the equations, the propagated error associated with the sources fractions terms (F) is from the variation of the C/N ratio and the $\delta^{13}C_{POC}$ of three end-members (river plume (RI), coastal nearshore water around DC channel (DC), and the *in situ* phytoplankton production (BIO)). The composite error propagation for fraction values (ε_F) can be expressed as a function of R_{RI}, R_{DC}, R_{BIO}, $\delta^{13}C_{POCRI}$, $\delta^{13}C_{POCDC}$, and $\delta^{13}C_{POCBIO}$, i.e., $f(R_{RI}, R_{DC}, R_{BIO}, \delta^{13}C_{POCRI}, \delta^{13}C_{POCDC}$, and $\delta^{13}C_{POCBIO})$, based on Taylor's expression (Han et al., 2012; Taylor, 1997):

$$\varepsilon_F = \frac{1}{n} \times \sqrt{\sum_i^n \left(\begin{array}{c} \left(\frac{\partial(f)}{\partial([R_{RI}]_i)} \times \delta([R_{RI}]_i) \right)^2 + \left(\frac{\partial(f)}{\partial([R_{DC}]_i)} \times \delta([R_{DC}]_i) \right)^2 + \left(\frac{\partial(f)}{\partial([R_{BIO}]_i)} \times \delta([R_{BIO}]_i) \right)^2 + \\ \left(\frac{\partial(f)}{\partial([\delta^{13}C_{POCRI}]_i)} \times \delta\left([\delta^{13}C_{POCRI}]_i\right) \right)^2 + \left(\frac{\partial(f)}{\partial([\delta^{13}C_{POCDC}]_i)} \times \delta\left([\delta^{13}C_{POCDC}]_i\right) \right)^2 + \left(\frac{\partial(f)}{\partial([\delta^{13}C_{POCBIO}]_i)} \times \delta\left([\delta^{13}C_{POCBIO}]_i\right) \right)^2 \end{array} \right)} \quad (6)$$

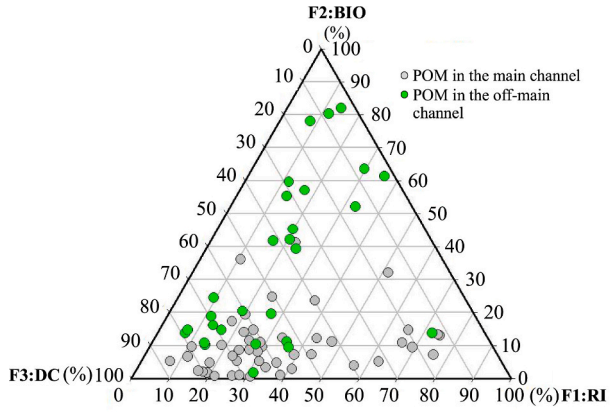

Fig. 7. The contributions of the three sources to particles, as calculated by the three end-member isotopic mixing model. Gray circles indicate samples collected along the main channel, while the green circles represent samples collected in the western off-main channel. (For interpretation of the references to colour in this figure legend, the reader is referred to the web version of this article.)

δ_i is the error propagation associated with the C/N ratios and the $\delta^{13}C_{POC}$ variation of the end-members, and n is the number of samples.

With the variations of the end-members of river plume and coastal nearshore water are 0.36‰ and 0.46‰ for $\delta^{13}C_{POC}$ values and 0.4 and 2.46 for C/N ratios, respectively, error propagation is calculated as 4% or less in the fractions (Table 2). The measured mean error of the C/N ratio, being 0.2, resulting from elemental analysis of 1% for POC and 5% for PN, has been considered in the error propagation estimation. The calculated alterations are much lower than the spatial deviation of the source fraction values. These points taken together, we contend that our results for source fraction values are reasonable.

4.2.2. Fractional contribution from different sources to POM

As illustrated in Fig. 7, the contributions of the three sources to the POM in Sansha Bay are determined. Riverine POM derived from the river plume and occupying the coastal seawater dominates along the main channel, accounting for about 35% and 55% of POM, respectively. In this area, the fraction of phytoplankton production in the main channel is as low as 10%. This suggested that the water mixing process between the river plume and the coastal nearshore water predominantly influenced the particle dynamics in the main channel, while the influence of POM sourced from the western bay was limited, probably due to the complex topography and slow water residence time. In the western off-main channel, the combined fractions of riverine POM from the main channel account for ~ 41%, with the river plume ~ 21% and DC channel ~ 20%, resulting from the limited tidal exchange and water mixing process. The dominant *in situ* phytoplankton production accounts for ~ 59%. These fractions are reasonable, given the flourishing of phytoplankton in the western bay, which could be fueled by abundant nutrient concentrations that may be derived from the POM degradation after migration, settlement, and accumulation, as the water residence time in the western bay is long.

4.3. POM dynamics and dissolved oxygen variation related to hydrological connectivity

4.3.1. Riverine POM degradation following Redfield respiration stoichiometry along the main channel

Based on a three isotopic end-member mixing model, the theoretical $\delta^{15}N_{PN}$ ($\delta^{15}N_{PNpre}$) in Sansha Bay was derived (Fig. 8a). Fig. 8a shows that the observed $\delta^{15}N_{PN}$ ($\delta^{15}N_{PN\,in\ situ}$) was much heavier than the $\delta^{15}N_{PNpre}$ in the main channel. This offset suggests that POM degradation probably releases lighter $\delta^{15}N$ preferentially and enriches heavier $\delta^{15}N$ in particles, as observed in previous studies (Savoye et al., 2003; Wu et al., 2003; Gruber, 2008; Casciotti, 2016; and references therein). Furthermore, POM degradation releases nitrogen first, reducing nitrogen content and elevating C/N ratio, together with riverine terrestrial plant origin POM in river plume which contained high C/N ratio,

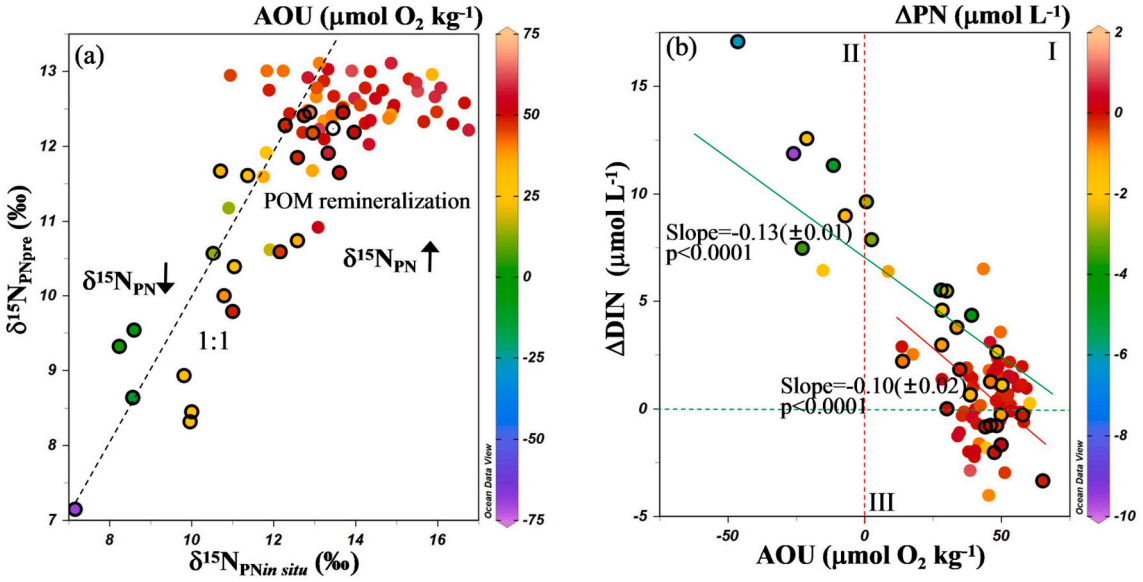

Fig. 8. (a) Scatter plots of $\delta^{15}N_{PNin\ situ}$ (‰) and $\delta^{15}N_{PNpre}$ (‰), as well as AOU (μmol O_2 kg^{-1}) in Sansha Bay. The dashed line indicates the 1:1 ratio. (b) Plots of the variation in dissolved inorganic nitrogen concentration (ΔDIN, μmol L^{-1}) vs. AOU (μmol O_2 kg^{-1}), overlaid with the variation in PN (ΔPN, μmol L^{-1}) in Sansha Bay. ΔDIN and ΔPN represent the differences between the conservative mixing prediction and the field measured values, respectively. They reflect the amount of DIN produced ("-") or removed ("+") and PN production ("-") or consumption ("+") associated with biogeochemical processes, as elaborated by Han et al. (Han et al., 2012, 2021). The green line indicates the relationship between ΔDIN and AOU when ΔDIN is consumed in quadrants I and II, indicating phytoplankton photosynthesis, with a slope of −0.13 ± 0.01. The red line represents the relationship between ΔDIN and AOU when AOU is consumed in quadrants I and III, indicating aerobic respiration, with a slope of −0.10 ± 0.02. The dots with black circles in (a) and (b) indicate the stations collected in the western off-main channel. (For interpretation of the references to colour in this figure legend, the reader is referred to the web version of this article.)

contribute higher C/N ratio in riverine POM as observed, consistent well with previous studies (Savoye et al., 2003; Wu et al., 2003; and references therein). Correspondingly, AOU, which represents oxygen utilization, displays a significant positive correlation along the main channel, indicating significant oxygen consumption during POM remineralization (Fig. 8a). On the other hand, decreasing ΔDIN has a clear negative correlation with increasing AOU. Although dissolved organic matter (DOM) decomposition might be an important DIN source (unfortunately we did not measure DOM), the significant negative correlation between ΔDIN and AOU, coupling with PN consumption (Fig. 8b), suggested that additional DIN may at least partly be produced by POM remineralization via aerobic respiration. In detail, the slope of ΔDIN vs. AOU in quadrants I and III where AOU >0 is 0.10 ± 0.02 ($p < 0.0001$), which is close to the classic Redfield stoichiometry (i.e., $DIN/O_2 = 16/138 = 0.12$, Redfield et al., 1963), and provided further evidence for the occurrence of aerobic respiration (Pilson, 2013). Additionally, the relationship between ΔDIP and AOU again shows a negative correlation, and the slope is 0.008 ± 0.001 ($p < 0.0001$, Fig. S2), which is also close to the classic Redfield ratio (i.e., $DIP/O_2 = 1/138 = 0.007$) and further indicated the rationality of POM remineralization. Note we acknowledge air-sea exchange process may affect the dynamics of DO concentration, AOU is positive and accompanied by negative ΔDIN (DIN production) even if AOU varies up to 50%, which implies the occurrence of POM remineralization. Synchronous consumption of oxygen and PN may suggest potential nitrification during aerobic respiration (Xu et al., 2022), which requires further study. Though DIN and/or nitrogen was regenerated, the utilization of those regenerated nutrients in the main channel may be weak, as indicated by low Chl *a* (< 4.5 mg m^{-3}) and low DIN consumption (ΔDIN ~ −1.0-2.0 μmol L^{-1}, Fig. S1 and Han et al., 2021). This is probably attributed to fast water mass mixing processes between riverine water and DC channel nearshore water (Figs. 2h, 8b), which are verified by significant DIN export flux via DC channel as estimated in our parallel study (Han et al., 2021; Lin et al., 2017). Briefly, along the main channel, riverine POM degraded via aerobic respiration and released nitrogen but with weak nitrogen assimilation due to fast water exchange.

4.3.2. *Feed food degradation, new PN production, and associated oxygen consumption and production in the western off-main channel*

In the western off-main channel, where the water residence time is longer (Lin et al., 2017), we observed a significant negative relationship between $\delta^{15}N_{PN}$ and Chl *a* ($p < 0.0001$, Fig. 5f). And low N/P ratio (~ 5.5–12) strongly suggests *in situ* phytoplankton production (Figs. 2f and 5f). Furthermore, we find a significant negative correlation between ΔDIN and AOU, which is consistent with the fact that phytoplankton production via photosynthesis induced DIN consumption and oxygen production. The slope of ΔDIN vs. AOU in quadrants I and II with positive ΔDIN, being 0.13 ± 0.01 ($p < 0.0001$, Fig. 8b), is consistent well with classic Redfield stoichiometry ($DIN/O_2 = 16/138 = 0.12$) and provided further evidence for the occurrence of *in situ* phytoplankton production (Pilson, 2013; Redfield et al., 1963).

On the other hand, similar to positive AOU and ΔPN in quadrants I and III along the main channel, some samples collected from the western off-main channel displayed POM remineralization via aerobic respiration, following the classic Redfield stoichiometry (Fig. 8b). Generally, the isotopic composition of regenerated ammonia ($\delta^{15}N_{NH4}$) may be heavier than that of nitrate ($\delta^{15}N_{NO3}$) during POM remineralization (York et al., 2010; Liu et al., 2018). In the western off-main channel, the observed $\delta^{15}N_{NH4}$ is ~10.5‰ ± 2.5‰, heavier than the value of $\delta^{15}N_{NO3}$ ~ 7.4‰ ± 0.8‰ (Table S1). Both $\delta^{15}N_{NH4}$ and $\delta^{15}N_{NO3}$ are comparable to the reported levels (i.e., $\delta^{15}N_{NH4}$ ~ 10.4‰ ± 0.5‰ in Waquoit Bay, Massachusetts, and $\delta^{15}N_{NO3}$ ~ 7‰ in Jiulong River, China) (Lin et al., 2022; York et al., 2010). Consistently, parts of $\delta^{15}N_{PNin\ situ}$ are slightly heavier than $\delta^{15}N_{PNpre}$ due to the release of lighter $\delta^{15}N$ during POM remineralization when AOU > 0 (Fig. 8a).

Noted that some $\delta^{15}N_{PNin\ situ}$ are slightly lighter than $\delta^{15}N_{PNpre}$ accompanied by negative AOU (Fig. 8a) in the western off-main channel, probably resulting from the uptake of regenerated nitrate and ammonia featured by lighter $\delta^{15}N$ during photosynthesis. This photosynthesis production is also characterized by negative ΔPN (PN added) and positive ΔDIN (DIN removed), matching well with the processes of PN production and DIN consumption. It is known that fish feed used in Sansha Bay is composed of ~ 90% fresh fish scrap and ~ 10% fodder (Han et al., 2021). The $\delta^{13}C_{POC}$ of fish feed is estimated to be −16.1‰ (= −15.3‰ × 90% + (−23.4‰ × 10%), Yokoyama et al., 2006), which agrees well with the $\delta^{13}C_{POC}$ of phytoplankton (Fig. 6b, Table 1). The $\delta^{15}N_{PN}$ of fish feed is estimated to be ~ 11.0‰ (=11.6‰ × 90% + 6.0‰ × 10%, Yokoyama et al., 2006), which is comparable to $\delta^{15}N_{NH4}$ in the water column (Fig. 6b, Table 1). These consistent isotopic compositions between fish feed (~ 11.0‰), ammonia (~ 10.5 ± 2.5‰), nitrate (~ 7.4‰ ± 0.8‰), and *in situ* phytoplankton (~ 7‰-12.5‰) imply the possibility of fish feed remineralization that coincides with the net isotope effect of ≤3‰ during particulate nitrogen remineralization and nitrogen utilization (Sigman et al., 2009). Thus, it is reasonable to speculate that the regenerated ammonia and nitrate with lighter $\delta^{15}N$ are probably sourced from fish food degradation after that stimulate phytoplankton production. This occurs during the processes of PN consumption and phytoplankton production, nitrogen regeneration and assimilation, and oxygen consumption and production in the western off-main channel (Figs. 6b and 8b), as well as potential nitrification and denitrification (Xu et al., 2022), require further study.

Our preliminary calculation on AOU shows that POM remineralization in the entire Sansha Bay water column overwhelmingly contributes to significant oxygen consumption (i.e., averaged AOU ~ 43.3 μmol O_2 kg^{-1}) and exceeds the amount of oxygen produced by phytoplankton production (i.e., averaged AOU ~ −27.5 μmol O_2 kg^{-1}) (Fig. 8). On benefit of the three end-member isotopic mixing model, the correlation between fraction of sources and AOU is built up (Fig. S3). We roughly estimate that the riverine POM fractions (i.e., $F_{RI} + F_{DC}$) need to be less than ~ 20% and/or the phytoplankton produced POM fraction (i.e., F_{BIO}) needs to be over ~ 80% to counter balance the consumed oxygen by POM remineralization (i.e., AOU ≤ 0) in the main channel and the off-main channel, respectively (Fig. S3).

5. Conclusion

This study has characterized the suspended particulates and sedimentary organic matter collected from Sansha Bay, a semi-closed bay suffering intensive mariculture in southeast China. Our results have provided detailed information on the concentrations and isotopic compositions of POC and PN, which indicate distinct POM features along the main channel and the western off-main channel, attributable primarily to hydrological water mixing processes and intrinsic biogeochemical processes.

Using POC, PN, and isotopic compositions of organic matter, we developed a well-validated, three end-member isotopic mixing model and quantitatively estimated the three major organic matter fractions in the integrated mariculture ecosystem (i.e., river plume, coastal nearshore water, and autochthonous phytoplankton production). Along the main channel, the riverine POM in the river plume (within Baima Harbor) and in the coastal nearshore water (around the DC channel) dominated at ~ 35% and ~ 55%, respectively, while phytoplankton production occupied only ~ 10%. On the other hand, autochthonous phytoplankton production contributed ~ 59%, whereas the riverine POM of the river plume and coastal nearshore contributed ~ 21% and ~ 20% in the western off-main channel.

Furthermore, significant remineralization of riverine POM overwhelmingly contributed to oxygen consumption along the main channel. Most of the regenerated nitrogen was transported out of the bay due to faster water exchange. Conversely, in the western off-main channel, *in situ* phytoplankton production and POM remineralization occurred concurrently. As indicated by the nitrogen isotopic signals, fish feed,

together with riverine POM exchanged from the main channel, may have degraded, thereby enhancing oxygen consumption and producing additional DIN. Regenerated nitrogen could stimulate phytoplankton production and complement a few oxygen concentrations in the western bay, given the slower water exchange time.

This study has significant implications for decision-making aimed at remediating the risk of eutrophication, hypoxia, and harmful algal blooms in similar semi-enclosed river-costal continuum areas in terms of mariculture intensity. The findings of this study will improve our systematic understanding of the impact of hydrological connectivity, mariculture activities, and intrinsic biogeochemistry on organic matter cycling in coastal bays and contribute to the development of sustainable coastal environments.

CRediT authorship contribution statement

Aiqin Han: Conceptualization, Methodology, Investigation, Writing – original draft. **Jin-Yu Terence Yang:** Formal analysis, Writing – original draft. **Mengli Chen:** Formal analysis, Writing – original draft. **Zhenzhen Zheng:** Formal analysis, Writing – original draft. **Xijie Yin:** Formal analysis. **Hui Lin:** Conceptualization, Formal analysis, Writing – original draft. **Min Nina Xu:** Formal analysis. **Shuh-Ji Kao:** Formal analysis, Writing – original draft.

Declaration of Competing Interest

The authors declare that they have no known competing financial interests or personal relationships that could have appeared to influence the work reported in this paper.

Data availability

Data will be made available on request.

Acknowledgments

This study was supported in part by the National Natural Science Foundation of China (grant No. 42103077), the Scientific Research Foundation of Third Institute of Oceanography, Ministry of Natural Resources, China (grant No. 2013017), and the Natural Science Foundation of Fujian Province of China (grant No. 2020J05077). The authors would like to express their gratitude to the crew of the R/V Minningyu F622 for their assistance during the cruise. Weifan Tang, Xiaowei Li, and Zhihong Lin assisted with sample collection, Xu Dong with dissolved oxygen measurement, Haili Yang with the dissolved inorganic nitrogen isotopic compositions measurement, while Yao Lai, Qiaoyun Lin, Lili Han, Wenbin Zou, and Li Tian assisted with POM and dual isotopic compositions determination. Constructive comments from three anonymous reviewers have greatly improved the quality of this study.

Appendix A. Supplementary data

Supplementary data to this article can be found online at https://doi.org/10.1016/j.aquaculture.2023.740109.

References

Andrews, J.E., Greenaway, A.M., Dennis, P.F., 1998. Combined carbon isotope and C/N ratios as indicators of source and fate of organic matter in a poorly flushed, tropical estuary: Hunts Bay, Kingston harbour, Jamaica. Estuar. Coast. Shelf Sci. 46, 743–756.

Benson, B.B., Krause Jr., D., 1984. The concentration and isotopic fraction of oxygen dissolved in freshwater and seawater in equilibrium with the atmosphere. Limnol. Oceanogr. 29 (3), 620–632.

Braman, R.S., Hendrix, S.A., 1989. Nanogram nitrite and nitrate determination in environmental and biological materials by vanadium (III) reduction with chemiluminescence detection. Anal. Chem. 61, 2715–2718. https://doi.org/10.1021/ac00199a00007.

Casciotti, K.L., 2016. Nitrogen and oxygen isotopic studies of the marine nitrogen cycle. Annu. Rev. Mar. Sci. 8, 379–407. https://doi.org/10.1146/annurev-marine-010213-135052.

Chang, J., Shiah, F.K., Gong, G.C., Chiang, K.P., 2003. Cross-shelf variation in carbon-to-chlorophyll a ratios in the East China Sea, summer 1998. Deep-Sea Res. II 50, 1237–1247.

Chen, C.-T.A., 2003. New vs. export production on the continental shelf. Deep-Sea Res. II. 50, 1327–1333.

Cifuentes, L.A., Sharp, J.H., Fogel, M.L., 1988. Stable carbon and nitrogen isotope biogeochemistry in the Delaware estuary. Limnol. Oceanogr. 33, 1102–1115.

Cifuentes, L.A., Coffin, R.B., Solorzano, L., Cardenas, W., Espinoza, J., Twilley, R.R., 1996. Isotopic and elemental variations of carbon and nitrogen in a mangrove estuary. Estuar. Coast. Shelf Sci. 43, 781–800.

Clawson, G., Kuempel, C.D., Frazier, M., Blasco, G., Cottrell, R.S., Froehlich, H.E., Metian, M., Nash, K.L., Többen, J., Verstaen, J., Williams, D.R., Halpern, B.S., 2022. Mapping the spatial distribution of global mariculture production. Aquaculture. 553, 738066.

Dagg, M., Ammerman, J., Amon, R.W., Gardner, W., Green, R., Lohrenz, S., 2007. A review of water column processes influencing hypoxia in the northern Gulf of Mexico. Estuar. Coasts 30, 735–752.

Dai, M., Guo, X., Zhai, W., Yuan, L., Wang, B., Wang, L., Cai, P., Tang, T., Cai, W., 2006. Oxygen depletion in the upper reach of the Pearl River estuary during a winter drought. Mar. Chem. 102, 159–169.

Dan, S.F., Liu, S.M., Yang, B., Udoh, E.C., Umoh, U., Ewa-Oboho, I., 2019. Geochemical discrimination of bulk organic matter in surface sediments of the Cross River estuary system and adjacent shelf, south East Nigeria (West Africa). Sci. Total Environ. 678, 351–368. https://doi.org/10.1016/j.scitotenv.2019.04.422.

Dong, S., Pan, K., Brockmann, U., 2000. Review on effects of mariculture on coastal environment. J. Ocean Univ. QingDao 30, 575–582 (in Chinese with English abstract).

Dubois, S., Savoye, N., Grémare, A., Plus, M., Charlier, K., Beltoise, A., Blanchet, H., 2012. Origin and composition of sediment organic matter in a coastal semi-enclosed ecosystem: an elemental and isotopic study at the ecosystem space scale. J. Mar. Syst. 94, 64–73.

Franco-Nava, M.-A., Blancheton, J.-P., Deviller, G., Le-Gall, J.-Y., 2004. Particulate matter dynamics and transformations in a recirculating aquaculture system: application of stable isotope tracers in seabass rearing. Aquac. Eng. 31, 135–155.

Fry, B., Wainright, S.C., 1991. Diatom sources of 13C-rich carbon in marine food webs. Mar. Ecol. Prog. Ser. 76, 149–157.

Gao, C., Yu, F., Chen, J., Hu, Z., Jiang, Y., Zhuang, Z., Xia, T., Kuehl, S.A., Zong, Y., 2021. Anthropogenic impact on the organic carbon sources, transport and distribution in a subtropical semi-enclosed bay. Sci. Total Environ. 767, 145047.

Gearing, J.N., Gearing, R.J., Rudrick, D.T., Requejo, A.G., Hutchins, M.J., 1984. Isotope variation of organic carbon in a phytoplankton based temperate estuary. Geochim. Cosmochim. Acta 48, 1089–1098.

Goericke, R., Fry, B., 1994. Variations of marine plankton $\delta^{13}C$ with latitude, temperature, and dissolved CO_2 in the world ocean. Glob. Biogeochem. Cycles 8, 85–90.

Gordon, E.S., Goñi, M.A., 2003. Sources and distribution of terrigenous organic matter delivered by the Atchafalaya River to sediments in the northern Gulf of Mexico. Geochim. Cosmochim. Acta 67 (13), 2359–2375.

Gruber, N., 2008. The marine nitrogen cycle: overview and challenges. In: Nitrogen in the Marine Environment. Elsevier Science & Technology, pp. 1–50.

Gu, Y., Ouyang, J., Ning, J., Wang, Z., 2017. Distribution and sources of organic carbon, nitrogen and their isotopes in surface sediments from the largest mariculture zone of the eastern Guangdong coast, South China. Mar. Pollut. Bull. 120, 286–291.

Han, A., Dai, M., Kao, S.-J., Gan, J., Li, Q., Wang, L., Zhai, W., Wang, L., 2012. Nutrient dynamics and biological consumption in a large continental shelf system under the influence of both a river plume and coastal upwelling. Limnol. Oceanogr. 57, 486–502.

Han, A., Kao, S.-J., Lin, W., Lin, Q., Han, L., Zou, W., Tan, E., Lai, Y., Ding, G., Lin, H., 2021. Nutrient budget and biogeochemical dynamics in Sansha Bay, China: A coastal bay affected by intensive mariculture. J. Geophys. Res.-Biogeosci. 126 https://doi.org/10.1029/2020JG006220 e2020JG006220.

Hargreaves, J.A., 1998. Nitrogen biogeochemistry of aquaculture ponds. Aquaculture. 166, 181–212.

Hatakeyama, Y., Kawahata, T., Fujibayashi, M., Nishimura, O., Sakamaki, T., 2021. Sources and oxygen consumption of particulate organic matter settling in oyster aquaculture farms: insights from analysis of fatty acid composition. Estuar. Coast. Shelf Sci. 254, 107328.

Hedges, J.I., Man, D.C., 1979. The characterization of plant tissues by their lignin oxidation products. Geochim. Cosmochim. Acta 43, 1803–1807.

Holligan, S.G., Montoya, J.P., Nevins, J.L., McCarthy, J.J., 1984. Vertical distribution and partitioning of organic carbon in mixed, frontal and stratified waters of the English Channel. Mar. Ecol. Prog. Ser. 14, 111–127.

Hu, J., Kawamura, H., Hong, H., Qi, Y., 2000. A review on the currents in the South China Sea: seasonal circulation, South China Sea warm current and Kuroshio intrusion. J. Oceanogr. 56, 607–624. https://doi.org/10.1023/a:1011117531252.

Hu, Z., Lee, J.W., Chandran, K., Kim, S., Khanal, S.K., 2012. Nitrous oxide (N_2O) emission from aquaculture: a review. Environ. Sci. Technol. 46, 6470–6480. https://doi.org/10.1021/es300110x.

Hu, B., Xie, M., Li, H., Zhao, W., Hu, J., Jiang, Y., Ji, W., Li, S., Hong, Y., Yang, M., Optiz, T., Shi, Z., 2022. Stoichiometry of soil carbon, nitrogen, and phosphorus in farmland soils in southern China: spatial pattern and related dominates. Catena. 217 https://doi.org/10.1016/j.catena.2022.106468.

Huang, D., Ding, G., 2014. Distribution feature and correlation analysis of COD in Sansha Bay. J. Fish. Res. 36, 453–458.
Jiang, Y., Guo, X., Sun, K., Rao, L., Li, J., Wang, L., Ye, Y., Li, W., 2017. Spatial variability of C-to-N ratio of farmland soil in Jiangxi Province. Environ. Sci. 38, 3840–3850 (in Chinese with English abstract).
Kao, S.-J., Lin, F.J., Liu, K.K., 2003. Organic carbon and nitrogen contents and their isotopic compositions in surficial sediments from the East China Sea shelf and the southern Okinawa trough. Deep-Sea Res. II. 50, 1203–1217.
Kao, S.-J., Shiah, F.K., Wang, C.H., Liu, K., K., 2006. Efficient trapping of organic carbon in sediments on the continental margin with high fluvial sediment input off southwestern Taiwan. Cont. Shelf Res. 26 (20), 2520–2537.
Kao, S.-J., Yang, J.-Y.T., Liu, K.-K., Dai, M., Chou, W.-C., Lin, H.-L., Ren, H., 2012. Isotope constraints on particulate nitrogen source and dynamics in the upper water column of the oligotrophic South China Sea. Glob. Biogeochem. Cycles 26. https://doi.org/10.1029/2011GB004091. GB2033.
Ke, Z., Chen, D., Liu, J., Tan, Y., 2020. The effects of anthropogenic nutrient inputs on stable carbon and nitrogen isotopes in suspended particulate organic matter in Jiaozhou Bay, China. Cont. Shelf Res. 208, 104244.
Knapp, A.N., Sigman, D.M., Lipschultz, F., 2005. N isotopic composition of dissolved organic nitrogen and nitrate at the Bermuda Atlantic time-series study site. Glob. Biogeochem. Cycles 19, 1–15. https://doi.org/10.1029/2004GB002320.
Li, F., Zhang, J., Mei, S., Li, N., 2009. The impact of farmland siol loss to water environment in Sansha Bay. Sci. Technol. Informat. 17, 746–747 (in Chinese with English abstract).
Lamb, A.L., Wilson, G.P., Leng, M.J., 2006. A review of coastal palaeoclimate and relative sea-level reconstructions using $\delta^{13}C$ and C/N ratios in organic material. Earth-Sci. Rev. 75 (1–4), 29–57.
Li, P., Lei, Y., Xie, H., Lu, J., 2014. Water pollution analysis and protection measures of drinking water sources of Jiaocheng section of Huotong River. J. Hengshui Univ. 16, 92–96 (in Chinese with English abstract). https://doi.org/10.3969/j.issn.1673-2065.2014.3901.3029.
Liénart, C., Susperregui, N., Rouaud, V., Cavalheiro, J., David, V., Del Amo, Y., Duran, R., Lauga, B., Monperrus, M., Pigot, T., Bichon, S., Charlier, K., Savoye, N., 2016. Dynamics of particulate organic matter in a coastal system characterized by the occurrence of marine mucilage-a stable isotope study. J. Sea Res. 116, 12–22.
Lin, H., Chen, Z., Hu, J., Cucco, A., Zhu, J., Sun, Z., Huang, L., 2017. Numerical simulation of the hydrodynamics and water exchange in Sansha Bay. Ocean Eng. 139, 85–94.
Lin, J., Krom, M.D., Wang, F., Cheng, P., Yu, Q., Chen, N., 2022. Simultaneous observations revealed the non-steady state effects of a tropical storm on the export of particles and inorganic nitrogen through a river-estuary continuum. J. Hydrol. 606, 127438. https://doi.org/10.121016/j.jhydrol.122022.127438.
Liu, K.-K., Kao, S.-J., 2007. A three end-member mixing model based on isotopic composition and elemental ratio. Terr. Atmos. Ocean. Sci. 18, 1067–1075. https://doi.org/10.3319/TAO.2007.1018.1065.1067(Oc.
Liu, K.-K., Wu, P.-C., 2014. Corrigendum to "A three end-member mixing model based on isotopic composition and elemental ratio". Terr. Atmos. Ocean. Sci. 25, 903.
Liu, Q., Kandasamy, S., Lin, B., Wang, H., Chen, C.-T.A., 2018. Biogeochemical characteristics of suspended particulate matter in deep chlorophyll maximum layers in the southern East China Sea. Biogeosciences 15, 2091–2109. https://doi.org/10.5194/bg-2015-2091-2018.
Lu, X., Huang, C., Chen, F., Zhang, S., Lao, Q., Chen, C., Wu, J., Jin, G., Zhu, Q., 2021. Carbon and nitrogen isotopic compositions of particulate organic matter in the upwelling zone off the east coast of Hainan Island, China. Mar. Pollut. Bull. 167, 112349. https://doi.org/10.1016/j.marpolbul.2021.112349.
Ma, Y., Wang, W., 2011. Carbon, nitrogen and phosphorus content and the ecological stoichiometric ratios of paddy field soil-plants in Minjiang River estuary. Subtrop. Agricult. Res. 7, 182–187 (in Chinese with English abstract).
Malet, N., Sauriau, P.-G., Ryckaert, M., Malestroit, P., Guillou, G., 2008. Dynamics and sources of suspended particulate organic matter in the Marennes-Oléron oyster farming bay: insights from stable isotopes and microalgae ecology. Estuar. Coast. Shelf Sci. 78, 576–586.
Malone, T.C., Newton, A., 2020. The globalization of cultural eutrophication in the coastal ocean: causes and consequences. Front. Mar. Sci. 7 https://doi.org/10.3389/fmars.2020.00670.
Martínez, M.L., Intralawan, A., Vázquez, G., Pérez-Maqueo, O., Sutton, P., Landgrave, R., 2007. The coasts of our world: ecological, economic and social importance. Ecol. Econ. 63, 254–272.
Martinotti, W., Camusso, M., Guzzi, L., Patrolecco, L., Pettine, M., 1997. C, N and their stable isotopes in suspended and sedimented matter from the PO estuary (Italy). Water Air Soil Pollut. 99, 325–332.
Meyers, P.A., 1994. Preservation of elemental and isotopic source identification of sedimentary organic matter. Chem. Geol. 114 (3–4), 289–302.
Middelburg, J.J., Levin, L.A., 2009. Coastal hypoxia and sediment biogeochemistry. Biogeosciences. 6, 1273–1293.
Middelburg, J.J., Nieuwenhuize, J., 1998. Carbon and nitrogen stable isotopes in suspended matter and sediments from the Schelde estuary. Mar. Chem. 60, 217–225.
Ming, Y., Gao, L., Guo, L., 2023. Dissolved and particulate organic carbon dynamics in the lower Changjiang River on timescales from seasonal to decades: response to climate and human impacts. J. Mar. Syst. 239, 103855.
Naik, H., Chen, C.-T.A., 2008. Biogeochemical cycling in the Taiwan Strait. Estuar. Coast. Shelf Sci. 78, 603–612. https://doi.org/10.1016/j.ecss.2008.1002.1004.
Pan, Z., Gao, Q., Dong, S., Wang, F., Li, H., Zhao, K., Jiang, X., 2019. Effects of abalone (*Haliotis discus hannai Ino*) and kelp (*Saccharina japonica*) mariculture on sources, distribution, and preservation of sedimentary organic carbon in Ailian Bay, China: identified by coupling stable isotopes ($\delta^{13}C$ and $\delta^{15}N$) with C/N ratio analyses. Mar. Pollut. Bull. 141, 387–397.
Pearson, T.H., Black, K.D., 2001. The environmental impacts of marine fish cage culture. In: Black, K.D. (Ed.), Environmental Impacts of Aquaculture. Sheffield Academic Press, Sheffield, pp. 1–31.
Pilson, M.E.Q., 2013. An Introduction to the Chemistry of the Sea, 2nd edition. Cambridge University Press, p. 213.
Redfield, A.C., Ketchum, B.H., Richards, F.A., 1963. The influence of organisms on the composition of seawater. In: Hill, M.N. (Ed.), The Sea, 2. John Wiley, pp. 26–77.
Riera, P., Richard, P., 1997. Temporal variation of $\delta^{13}C$ in particulate organic matter and oyster Crassostrea gigas in Marennes-Oléron Bay (France): effect of freshwater inflow. Mar. Ecol. Prog. Ser. 147, 10515.
Rožič, P.Ž., Dolenec, T., Lojen, S., Kniewald, G., Dolenec, M., 2014. Using stable nitrogen isotopes in Patella sp. to trace sewage-derived material in coastal ecosystems. Ecol. Indic. 36, 224–230.
Samanta, P., Shin, S., Jang, S., Song, Y.C., Oh, S., Kim, J.K., 2019. Stable carbon and nitrogen isotopic characterization and tracing nutrient sources of Ulva blooms around Jeju coastal areas. Environ. Pollut. 254, 113033.
Sarà, G., Scilipoti, D., Mazzola, A., Modica, A., 2004. Effects of fish farming waste to sedimentary and particulate organic matter in a southern Mediterranean area (gulf of Castellammare, Sicily): a multiple stable isotope study ($\delta^{13}C$ and $\delta^{15}N$). Aquaculture. 234, 199–213.
Savoye, N., Aminot, A., Treguer, P., Fontugne, M., Naulet, N., Kerouel, R., 2003. Dynamics of particulate organic matter $\delta^{15}N$ and $\delta^{13}C$ during spring phytoplankton blooms in a macrotidal ecosystem (bay of seine, France). Mar. Ecol. Prog. Ser. 255, 27–41.
Shultz, D.J., Calder, A., 1976. Organic carbon $^{13}C/^{12}C$ variations in estuarine sediments. Geochim. Cosmochim. Acta 40, 381–385.
Sigman, D.M., Casciotti, K.L., Andreani, M., Barford, C., Galanter, M., Böhlke, J.K., 2001. A bacterial method for the nitrogen isotopic analysis of nitrate in seawater and freshwater. Anal. Chem. 73, 4145–4153. https://doi.org/10.1021/ac010088e.
Sigman, D.M., Karsh, K.L., Casciotti, K.L., 2009. Ocean process tracers: nitrogen isotopes in the ocean. Encycloped. Ocean Sci. 40–54 (2nd edition). Academic Press. https://doi.org/10.1016/B1978-012374473-012374479.012300632-012374479.
Swarzenski, P.W., Campbell, P.L., Osterman, L.E., Poore, R.Z., 2008. A 1000-year sediment record of recurring hypoxia off the Mississippi River: the potential role of terrestrially-derived organic matter inputs. Mar. Chem. 109, 130–142.
Taylor, J.R., 1997. An Introduction to Error Analysis, 2nd ed. University Science Books.
Thomas, H., Bozec, Y., Elkalay, K., Baar, H.J.D., 2004. Enhanced open ocean storage of CO_2 from shelf sea pumping. Science. 304, 1005–1008.
Vizzini, S., Mazzola, A., 2006. The effects of anthropogenic organic matter inputs on stable carbon and nitrogen isotopes in organisms from different trophic levels in a southern Mediterranean coastal area. Sci. Total Environ. 368, 723–731.
Vizzini, S., Savona, B., Caruso, M., Savona, A., Mazzola, A., 2005. Analysis of stable carbon and nitrogen isotopes as a tool for assessing the environmental impact of aquaculture: a case study from the western Mediterranean. Aquac. Int. 13, 157–165.
Wada, E., Minagawa, M., Mizutani, H., Tsuji, T., Imaizumi, R., Karasawa, K., 1987. Biogeochemical studies on the transport of organic matter along the Otsuchi River watershed, Japan. Estuar. Coast. Shelf Sci. 25, 321–336.
Wang, Y.G., Song, Z.R., Jiang, C.L., Kong, J., Liu, Q., 2009. In: Liu, X.D. (Ed.), Study of Modeling and Environment of Bays in Fujian Province-Sansha Bay. China Ocean Press.
Wang, H., Dai, M., Liu, J., Kao, S.-J., Zhang, C., Cai, W.-J., Wang, G., Qian, W., Zhao, M., Sun, Z., 2016. Eutrophication-driven hypoxia in the East China Sea off the Changjiang estuary. Environ. Sci. Technol. 50, 2255–2263. https://doi.org/10.1021/acs.est.2255b06211.
Welschmeyer, N.A., 1994. Fluorometric analysis of chlorophyll a in the presence of chlorophyll b and pheopigments. Limnol. Oceanogr. 39 (8), 1985–1992.
Wu, Y., Zhang, J., Li, D.J., Wei, H., Lu, R.X., 2003. Isotope variability of particulate organic matter at the PN section in the East China Sea. Biogeochemistry. 65, 31–49.
Xie, B., Huang, J., Huang, C., Wang, Y., Shi, S., Huang, L., 2020a. Stable isotopic signatures ($\delta^{13}C$ and $\delta^{15}N$) of suspended particulate organic matter as indicators for fish cage culture pollution in Sansha Bay, China. Aquaculture. 522.
Xie, G., Lou, X., Ruan, Y., Tong, X., Xu, J., 2020b. Characteristic and influencing factors of C/N ratio of farmland soil in Zhejiang Province. Acta Agricult. Jiangxi. 32, 51–55 (in Chinese with English abstract).
Xu, M.N., Wu, Y., Zheng, L., Zheng, Z., Zhao, H., Laws, E.A., Kao, S.-J., 2017. Quantification of multiple simultaneously occurring nitrogen flows in the euphotic ocean. Biogeosciences 1021–1038. https://doi.org/10.5194/bg-1014-1021-2017.
Xu, M.N., Wu, Y., Zhang, X., Tang, J.-M., Tan, E., Zheng, Z.-Z., Du, M., Yan, X., Kao, S.-J., 2022. Diel change in inorganic nitrogenous nutrient dynamics and associated oxygen stoichiometry along the Pearl River. Estuary Water Res. 222, 118954. https://doi.org/10.1016/j.watres.2022.118954.
Yang, J.-Y.T., Kao, S.-J., Dai, M., Yan, X., Lin, H.-L., 2017. Examining N cycling in the northern South China Sea from N isotopic signals in nitrate and particulate phases. J. Geophys. Res.-Biogeosci. 122, 2118–2136.
Yokoyama, H., Abo, K., Ishihi, Y., 2006. Quantifying aquaculture-derived organic matter in the sediment in and around a coastal fish farm using stable carbon and nitrogen isotope ratios. Aquaculture. 254, 411–425.
York, J.K., Tomasky, G., Valiela, I., Giblin, A.E., 2010. Isotopic approach to determining the fate of ammonium regenerated from sediments in a eutrophic sub-estuary of Waquoit Bay, MA. Estuar. Coasts 33, 1069–1079.
Yu, Z.T., Wang, X.J., Zhang, E.L., Zhao, C.Y., Liu, X.Q., 2015. Spatial distribution and sources of organic carbon in the surface sediment of Bosten Lake, China. Biogeosciences. 12 (22), 6605–6615.

Zhang, L., Altabet, M.A., Wu, T., Hadas, O., 2007. Sensitive measurement of NH_4^+ $^{15}N/^{14}N$ ($\delta^{15}N_{NH4}$) at natural abundance levels in fresh and saltwaters. Anal. Chem. 79, 5297–5303.

Zhu, Z.Y., Zhang, J., Wu, Y., Zhang, Y.Y., Lin, J., Liu, S.M., 2011. Hypoxia off the Changjiang (Yangtze River) estuary: oxygen depletion and organic matter decomposition. Mar. Chem. 2011, 108–116.

Zhu, F., Shi, Z., Ling, X., Xia, Y., Li, Y., Weng, Y., Liu, Y., 2013. Relationship between cage aquaculture and environmental quality in Sansha Bay of Ningde. Mar. Sci. Bull. 32, 171–177 (in Chinese with English abstract).